SELECTING FILTER MEDIA FOR PHOSPHORUS REMOVAL AT THE ENNIS NATIONAL FISH HATCHERY THREE-STAGE SUBSURFACE FLOW TREATMENT WETLAND

by

Jack Enoch Wallis

A thesis submitted in partial fulfillment
of the requirements for the degree

of

Master of Science

in

Environmental Engineering

MONTANA STATE UNIVERSITY
Bozeman, Montana

July 2017

©COPYRIGHT

by

Jack Enoch Wallis

2017

All Rights Reserved

TABLE OF CONTENTS

1. INTRODUCTION 1

2. DESIGN AND OPERATION OF A TREATMENT WETLAND SYSTEM AT THE ENNIS NATIONAL FISH HATCHERY 6

System Design 8
Wastewater Collection System 10
System Hydraulic Design 11
Stage 1 Wetland Design 13
Stage 2 Wetland Design 16
Stage 3 Wetland Design 18
Control System 19
Startup Operation and Sampling Methods 19
Operation 19
Sampling 21
Water Quality Analysis 21
Results and Discussion 22
Hydraulic Loading 22
Pilot System Water Quality Results 23
Full-Scale System Water Quality Results 24

3. SELECTING WETLAND MEDIA FOR PHOSPHORUS REMOVAL 31

Contribution of Authors and Co-Authors 31
Manuscript Information Page 32
Introduction 33
Literature review 34
Phosphorus Cycle 35
Phosphorus Removal in Subsurface Flow Treatment Wetlands 38
Plant Uptake 38
Sedimentation and Filtration 39
Adsorption 40
Phosphorus Adsorption Mechanisms 44
Factors Influencing Phosphorus Adsorption 47
Water Chemistry 48
Operational Parameters 51
Materials and Methods 52
Materials 52
Batch Adsorption Tests 53
Column Tests 56
Water Quality Analysis 60
Statistical Analysis 60

TABLE OF CONTENTS CONTINUED

Results 61
Media Characteristics 61
Batch Adsorption Isotherms 63
Adsorption Isotherm Equations 66
Precipitation in Blaine Spring Creek Water 75
Continuous Flow Tests 77
Discussion 83
Effect of Media Characteristics 83
Effect of Water Quality 87
Performance of Continuous Flow Columns 90
Batch versus Column Results 91
Column Removal Kinetics 95

4. CONCLUSIONS AND RECOMMENDATIONS 98

REFERENCES CITED 102

LIST OF TABLES

Table Page

1. Treatment wetland sizing criteria, design loading, and size. 10
2. Pilot-scale wetland water quality results..... 24
3. Full-scale wetland water quality results..... 24
4. Design parameters versus actual values for flow, HLR, stage 1 TSS load, stage 2 recycle rate, stage 2 COD load, and stage 2 TN load. 29
5. Media to solution ratios for each media in adsorption isotherm experiments. 54
6. Elemental composition of mineral media. 62
7. pH of media in DI and BSC water. 63
8. Maximum adsorption capacity, Langmuir, and Freundlich coefficients. 67
9. Column hydraulic residence time. 78
10. Phosphorus removal in column experiments attributed to each material compared to phosphorus removal in batch tests at a similar P concentration. 93
11. Utelite column modified first order reaction kinetics. 96

LIST OF FIGURES

Figure Page

1. Location of the ENFH and receiving water bodies. 2

2. Treatment wetland flow schematic. Dashed lines represent components not used under normal operations. 9

3. Wastewater vacuum head attached to 2-inch rigid PVC handle in raceway quiescent zone. PVC handle is attached the vacuum header via flexible tubing (not shown). 11

4. Stage 1 wetland cell valve distribution box (A), cells prior to plant establishment (B), and underdrain piping prior to fill with media. Vertical gray pipes in (B) are distribution lines, white pipes are vent pipes connected to drain lines. 15

5. Stage 1 wetland cell cross section. 15

6. Stage 2 wetland cell cross section. 17

7. Nutrient removal cells prior to plant establishment. Vertical white pipes are vent lines connected to drainage piping. 17

8. Stage 3 wetland cell cross section. 18

9. Phosphorus removal bed tanks prior to filling with media. 18

10. Daily cleaning volumes. Stars show days when grab samples were collected. 23

11. Average organic nitrogen, ammonia, nitrate, and nitrite concentrations in grab samples taken from the settling tank (ST), recycle tank (RT) and transfer tank (TT). 26

12. Average total phosphorus and orthophosphate in grab samples taken from the settling tank (ST), recycle tank (RT) and transfer tank (TT). 28

13. Stage 1 wetland cell on May 10, 2017. Lighter regions on left and right sides show areas with no solids layer. Established plants are just breaking winter dormancy. 30

LIST OF FIGURES CONTINUED

Figure Page

14. Phosphorus cycle in subsurface flow treatment wetlands. Green arrows indicate biological processes and red arrows indicate abiotic processes. 36

15. Solubility of strengite (iron phosphate), variscite (aluminum phosphate), DCP (dicalcium phosphate), ACP1 and ACP2 (amorphous calcium phophates), and HAP (hydroxyapatite). Modified from Stumm and Morgan (1996). 50

16. Configuration of column experiments. 58

17. Adsorbed P versus equilibrium aqueous P concentration of all coarse size fraction media tested in DI water. Error bars represent standard error (n=3). 64

18. Adsorbed P versus equilibrium aqueous P concentration of all coarse size fraction media tested in BSC water. Error bars represent standard error (n=3). 65

19. Adsorbed P versus equilibrium aqueous P concentration of coarse and fine Utelite in DI water, and coarse Utelite in BSC water. Error bars represent standard error (n=3). 68

20. Adsorbed P versus equilibrium aqueous P concentration of coarse and fine limestone in DI water, and coarse limestone in BSC water. Error bars represent standard error (n=3)..... 70

21. Adsorbed P versus equilibrium aqueous P concentration of coarse and fine shale in DI water, and coarse shale in BSC water. Error bars represent standard error (n=3)..... 71

22. Adsorbed P versus equilibrium aqueous P concentration of coarse gravel in DI water and BSC water. Lines represent fitted Langmuir isotherm curves. Error bars represent standard error (n=3). 72

23. Adsorbed P versus equilibrium aqueous P concentration of coarse dolomite in DI water, with Langmuir isotherm curve. Error bars represent standard error (n=3)..... 73

LIST OF FIGURES CONTINUED

Figure Page

24. Adsorbed P versus equilibrium aqueous P concentration of coarse juniper biochar in BSC water with Langmuir isotherm curves. Error bars represent standard error (n=3). 74

25. Adsorbed P versus equilibrium aqueous P concentration of coarse lodgepole biochar in BSC water with Langmuir isotherm curves. Error bars represent standard error (n=3)..... 75

26. Ratio of equilibrium P to initial P versus initial P concentration in BSC water (without media). 76

27. Column influent and effluent P concentrations. Vertical dashed line represents transition between phase 1 and phase 2 in the Utelite columns. 80

28. Column influent and effluent pH. Horizontal dashed line shows typical discharge pH limit of 9. Vertical dashed line represents transition between phase 1 and phase 2 in Utelite columns..... 81

29. Cumulative P removed versus cumulative P added, normalized to the column reactor volume. Vertical dashed line represents average point of transition between phase 1 and phase 2 (range 93 – 135 mg P/L reactor volume). 83

30. Relationship between calcium, iron, magnesium, and aluminum content on maximum adsorption capacity of Utelite (UT), limestone (LS), shale (SH), gravel (GR), and dolomite (DO). Maximum adsorption capacities for each set of batch experiments performed with each media are shown (fine media in DI water, coarse media in DI water, coarse media in BSC water)..... 85

31. Equilibrium pH of batch adsorption tests in DI water. 89

32. Equilibrium pH of batch adsorption tests in BSC water. 90

33. Phosphorus removal efficiency of layered Utelite columns (A) and mixed Utelite columns (B) versus HRT with k-C* model fit to the data of 22-34 pore volumes..... 96

ABSTRACT

In western Montana, phosphorus is one of the most common contaminants found in rivers and streams, threatening the health of aquatic ecosystems. In response to growing water quality concerns and new regulatory requirements, a three-stage treatment wetland was recently constructed at the Ennis National Fish Hatchery to treat wastewater generated by raceway cleaning operations. Currently only the first two stages of this system are complete and over the first two months of operation have removed over 98% of influent chemical oxygen demand, 99% of total suspended solids, 59% of total nitrogen, and 95% of total phosphorus. However, the effluent phosphorus concentration is expected to increase as organic matter accumulating in the wetland mineralizes and the phosphorus adsorption capacity of the wetland media is saturated. To maintain long-term phosphorus removal, the treatment wetland was designed with a filter unit to be filled with media capable of adsorbing large quantities of phosphorus. The purpose of this research is to choose the optimal media for this filter unit, comparing three manufactured materials (lightweight aggregate, juniper biochar, and lodgepole biochar) and four natural materials (limestone, dolomite, shale, and gravel). Batch adsorption experiments were conducted with coarse media in deionized water, coarse media in Blaine Spring Creek water, and fine media in deionized water. The difference between these batch experiments showed that water chemistry and particle size significantly affect phosphorus adsorption for a given material. Based on their high performance in batch experiments, lightweight aggregate and lodgepole biochar were tested in continuous flow columns, along with gravel to provide a baseline performance comparison. Gravel and lightweight aggregate removed more phosphorus in continuous flow columns than in batch experiments, likely due to ongoing precipitation with calcium ions in the influent. Lightweight aggregate was the top performing media in all experiments, and is recommended for use in the filter units at the Ennis National Fish Hatchery treatment wetland. Based on its phosphorus removal capacity in column experiments (1200 mg P kg^{-1} lightweight aggregate), the filter beds will be saturated in 14 months if the current effluent phosphorus concentration of 2.3 mg L^{-1} is maintained.

INTRODUCTION

In the western mountain region of Montana, phosphorus (P) is the most widespread contaminant found in rivers and streams, with nearly forty percent containing elevated levels (Cramer Fish Sciences, 2013). As a limiting nutrient in most aquatic ecosystems, high phosphorus concentrations can result in increased growth of aquatic plants and algae. If excessive, this growth can cause eutrophication of the water body, creating negative ecological and human impacts. The ecological degradation associated with eutrophication is multi-faceted: decomposition of plant biomass can deplete oxygen concentrations, interfering with fish and invertebrate growth; excessive algae can damage invertebrates; and excessive phosphorus is associated with declines in invertebrate community structure (U.S. EPA, 2016). Increases in aquatic plants and algae can also affect human uses – from aesthetics to recreation. Reducing phosphorus discharges into natural water bodies is therefore a priority for protecting water quality. From an engineering perspective, limiting phosphorus in wastewater effluent is a key piece of this puzzle.

The Ennis National Fish Hatchery (ENFH) is a large trout hatchery located at the head of Blaine Spring Creek, a small tributary to the Madison River south of Ennis, Montana (Figure 1). Blaine Spring Creek flows at rate of approximately 0.9 cubic meters per second ($m^3\ s^{-1}$), and much of this water is diverted directly from the spring box of Blaine Spring, passes through the hatchery, and is discharged downstream. Hatchery effluent is generally high quality, but solids that settle on raceway floors must be periodically removed to protect fish health. Historically, this was accomplished by

increasing raceway water velocity, flushing solids to Blaine Spring Creek. Hatchery effluent did not undergo treatment prior to discharge, but due to the high flow rates and infrequent flushing, negative environmental effects were not readily apparent. However, fish hatchery solids contain high concentrations of carbon, nitrogen, and phosphorus, and due to the small size of Blaine Springs Creek and the high contaminant mass load of approximately 7,400 kilograms (kg) of solids per year, limiting this nutrient load is important to protect water quality. In response to growing awareness of water quality issues and new regulatory requirements prohibiting the discharge of raceway solids into receiving water bodies, the ENFH installed a wastewater collection and treatment system to remove and treat raceway solids in 2015-2016.

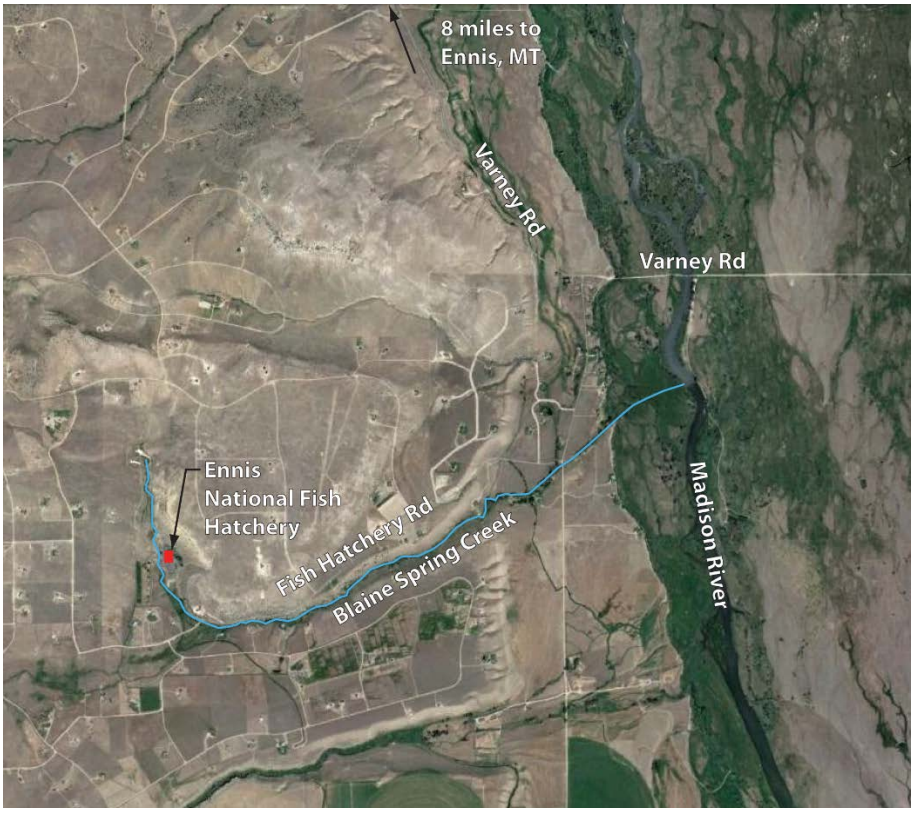


Figure 1. Location of the ENFH and receiving water bodies.

A three-stage treatment wetland (TW) system was chosen to treat raceway solids, designed by the Treatment Wetlands Research Group in the Civil Engineering Department at Montana State University. Treatment wetlands have been shown to be highly effective in improving water quality from a variety of sources, ranging from high strength agricultural wastewaters to highly treated municipal secondary effluent (Kadlec & Wallace, 2009). These systems typically have much lower capital and operating costs compared to traditional treatment systems, at the expense of greater land area requirements. This makes them ideal for small scale systems in rural areas, such as the ENFH, where financial resources available for wastewater treatment are limited, but land area is available.

While design standards and operational strategies are well established for carbon and nitrogen removal, phosphorus removal in treatment wetlands remains a challenge (Vohla et al., 2011; Vymazal, 2007). This is because unlike nitrogen and carbon, the gas phase is only a small fraction of the phosphorus cycle, and therefore aqueous phosphorus must be transformed to a solid phase to be removed from wastewater. Due to the difficulty in achieving this, TWs show mixed efficacy in removing P, with certain types of TW's performing better than others. Treatment wetlands can be classified as either free water surface (FWS) wetlands, in which water flows above the surface of the wetland media, or subsurface flow (SSF) wetlands, in which water flows through the wetland media. Subsurface flow wetlands are further divided into either horizontal flow (HSSF) or vertical flow (VF) configurations. Free water surface wetlands have a long history of successful P removal through the accumulation of P containing sediments (Kadlec &

Wallace, 2009). However, this requires significantly more land area than subsurface flow wetlands, and while land is available at the ENFH, it is insufficient for large P removing FWS wetlands. The ENFH treatment wetland is designed as a SSF wetland, with two VF stages to take advantage of their high aerobic capacity, and a HSSF stage to be used for phosphorus removal.

Phosphorus removal in SSF wetlands occurs primarily through adsorption onto wetland media, with incorporation into plant biomass playing a substantial role in certain circumstances. Because these phosphorus pools become saturated over time, long-term phosphorus removal remains a challenge (Vohla et al., 2011). In addition, adsorption depends largely upon water quality and wetland media characteristics, making predicting and maximizing phosphorus removal in new TWs difficult. Despite a large body of literature describing successful phosphorus removal in SSF wetlands (Heistad et al., 2006; Hill et al., 2000; Jenssen & Krogstad, 2003; Öövel et al., 2007; Shilton et al., 2006), direct application of this research to new systems is often difficult due to differences between studied and local systems, particularly local water quality and available wetland media. Therefore, regional knowledge of available media and water quality is critical for maximizing phosphorus removal in newly constructed TWs.

The goal of the research in this thesis is twofold: to characterize the preliminary operation of the vertical flow components of ENFH treatment wetland system and to test appropriate, locally sourced filter media options to maximize phosphorus removal for eventual use in the HSSF component. This thesis is organized into three main chapters. In Chapter 2, the ENFH treatment wetland system is described, and the results of a pilot

system and preliminary full-scale operation are presented. Chapter 3 focuses on options for an appropriate filter media for P removal at the ENFH treatment wetland. This chapter is organized for submission to an appropriate refereed journal and includes a literature review of P removal in treatment wetlands and the results of laboratory experiments on potential filter media. In Chapter 4, recommendations for the optimal P filter media based on the results of previous sections, and implications for P removal at the ENFH treatment wetland are discussed.

DESIGN AND OPERATION OF A TREATMENT WETLAND SYSTEM AT THE ENNIS NATIONAL FISH HATCHERY

The ENFH is a broodstock hatchery, specializing in raising rainbow trout to adult size and harvesting their eggs to be shipped to production hatcheries, where the trout are raised to stockable sizes. The hatchery has 38 hatchery tanks, 48 circular tanks, and 36 raceways, producing approximately 20 million rainbow trout eggs per year. Trout hatcheries require a high flow rate of clean water to prevent buildup of ammonia, which is toxic to the fish. The hatchery takes approximately 5,450 cubic meters per day (m^3/d) directly from a spring box feeding the creek, and water takes a single pass through the hatchery prior to discharge. This results in a high effluent flow rate with low average contaminant concentrations. However, solids consisting of fish waste and uneaten food settle to the bottom of raceways, and must be removed.

Prior to 2011, the Montana Department of Environmental Quality (DEQ) did not set effluent treatment requirements for fish hatcheries, thus the ENFH did not have any effluent treatment facilities. Solids were removed by periodically flushing the raceways and all flushed solids entered Blaine Springs Creek. In 2011, the DEQ renewed the Concentrated Aquatic Animal Production (CAAP) General Permit, requiring effluent treatment for facilities producing more than 20,000 pounds of fish per year, and prohibiting direct discharge of solids to state waters. Due to the high flow rates, low pollutant concentrations, and high temporal variation in water quality, setting concentration-based discharge requirements for fish hatcheries is difficult. Instead, the CAAP General Permit requires hatcheries to develop best management practices (BMP's)

to limit waste discharges to state waters, including methods to capture and remove accumulated raceway solids.

To meet these permit requirements, the ENFH constructed a wastewater system consisting of two components: a wastewater collection system to remove raceway solids, and a wastewater treatment system to treat the solids. The collection system includes a water vacuum to remove the settled solids from the raceway floors, pumping the vacuumed wastewater to the treatment system. The wastewater is highly concentrated compared to the total hatchery effluent, allowing the treatment system to be designed for a much lower flow rate than the total hatchery flow. For the first three months of operation the treatment system received an average of 4 m^3 d^{-1}, less than 0.1% of the total hatchery flow of 5450 m^3 d^{-1}.

The treatment system consists of two vertical flow wetland stages followed by a horizontal flow stage. The vertical flow stages were designed based on the French system, which is currently the state of the art in municipal wastewater treatment wetlands (Molle et al., 2005; Paing et al., 2015). The French system has been shown to be highly effective in removing suspended solids, chemical oxygen demand (COD), and ammonia nitrogen, and shows promise for total nitrogen removal. The third horizontal flow stage was designed for phosphorus removal, and design of this stage is the focus of the research in this thesis. A pilot wetland system was constructed and operated in 2014 to verify the feasibility and sizing criteria, and construction on the full-scale system began in 2015. A preliminary startup began with the operation of the first stage of the system in August 2016, meeting an extended deadline for the CAAP General Permit. Construction of the

first two stages was completed in March 2017. The third stage has remained unused, as the filter media to fill the wetland cells is to be selected based on this research.

This chapter includes a detailed description of the treatment wetland design and operation, with a focus on the vertical flow components. The results of the pilot system and preliminary full-scale operations are presented, including a characterization of influent and effluent wastewater.

System Design

As discussed previously, the ENFH wastewater system is composed of two primary components: the collection system, and a three-stage treatment wetland system (Figure 2). Although this thesis focuses on the treatment system, it is important to recognize that wastewater quantity and quality depends greatly upon hatchery operations, particularly operation of the collection system. Wastewater is sent from the collection system to either the Stage 1 wetland cells or a settling tank, both of which are designed to remove suspended solids. From there, wastewater flows to a recycle tank where it is pumped to the stage 2 wetland cells, designed to remove COD and nitrogen. Effluent from the second stage can be recycled back through the second stage but is eventually pumped to the stage 3 cells, designed to remove phosphorus.

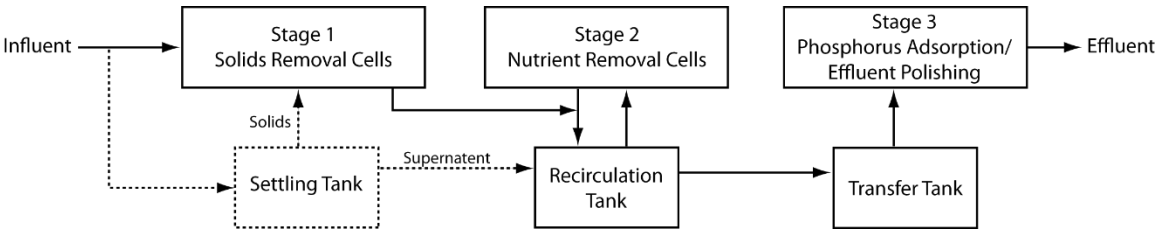


Figure 2. Treatment wetland flow schematic. Dashed lines represent components not used under normal operations.

Design criteria for the treatment wetland was based on the latest information available from literature and experience operating a similar wetland system at the Bridger Bowl Ski Area. Loading rates were determined based on the results of a pilot wetland, which operated over three months in late summer and fall of 2014. The pilot wetland consisted of three scaled down stage 1 wetland cells, each with a surface area of 2.6 m^2 and with similar cross sectional design to the stage 1 cells described below. The full-scale stage 1 and 2 wetlands were sized based on the design sizing criteria and loading rates shown in Table 1. The stage 1 solids loading was estimated as 20% of the total hatchery feed mass in 2014. The flow rate was estimated based on an assumed maximum daily cleaning volume 18.9 $m^3\ d^{-1}$; assuming five days of cleaning per week, this results in an average flow rate of 13.5 $m^3\ d^{-1}$. The stage 2 COD and TN loading rates were estimated based on this average flow rate and estimated stage 1 effluent concentrations of 200-500 mg COD L^{-1} and 15 mg TN L^{-1}. Because phosphorus removal was not the primary treatment goal, P concentrations were not measured during operation of the pilot system, and sizing criteria for stage 3 was developed during this research. The design of each system component is elaborated further below.

Table 1. Treatment wetland sizing criteria, design loading, and size.

Design Parameter	Sizing Criteria	Design Loading	Required Size
TSS (Stage 1)[1]	50 kg m^{-2} yr^{-1}	7400 kg yr^{-1}	148 m^2
COD (Stage 2)	40 g m^{-2} d^{-1}	2700-6750 g d^{-1}	67 – 168 m^2
TN (Stage 2)	2.7 g m^{-2} d^{-1}	203 g d^{-1}	75 m^2

1. Parentheses indicate the stage which the design parameter applies to.

Wastewater Collection System

The wastewater collection system is composed of a self-priming pump (Gorman-Rupp T2A60-B /F) with a variable speed drive in each raceway building attached to a vacuum header line. The pumps are capable of flow up to 100 gallons per minute (gpm), and are typically set to approximately 30 – 60 gpm; the flow rate varies significantly during cleaning as the system head loss depends upon the proximity of the vacuum head to the floor. The vacuum header line extends the length of the raceway building, with six equally spaced risers near the ends of the raceways. Each riser has a ball valve and terminates in a cam-lock fitting, allowing a flexible hose with the vacuum head to be attached (Figure 3). The vacuum head is then used to remove solids from raceway floors.

Due to the turbulence caused by swimming fish, most of the solids settle in the quiescent zone of each raceway (Figure 3). Typically, only the quiescent zone is vacuumed, unless a significant portion of solids accumulate in the upper raceways, in which case the whole raceway or a portion is vacuumed. Solids may accumulate due to spillage, overfeeding, or under-eating while the trout are becoming accustomed to a new food source. The quantity and concentration of solids in the wastewater produced by the vacuum system therefore depends upon total hatchery production, fish life cycle, cleaning

frequency, cleaning duration, and general operational characteristics (i.e. leaving vacuum head in water to capture cleaner water without solids).



Figure 3. Wastewater vacuum head attached to 2-inch rigid PVC handle in raceway quiescent zone. PVC handle is attached the vacuum header via flexible tubing (not shown).

System Hydraulic Design

Wastewater is sent from the collection system either directly to the first stage of the wetland system, or to a settling tank. The settling tank is 3.2 m deep with an effective volume of 21 m^3, and is sized to retain solids through the winter if cold weather prevents the use of the first stage. A 40 gallon per minute (gpm) submersible pump (Goulds WE0512HH) can pump wastewater to the stage 1 cells if the settling tank is being used. Water can drain back through the pump to prevent pipe freezing. An overflow pipe at 2.8

m allows supernatant from the settling tank to flow into a second 21 m^3 tank (recycle tank). Wastewater also drains from the stage 1 cells into the recycle tank. An overflow pipe is connected to the stage 1 effluent pipe just prior to entering the recycle tank, which allows both the settling tank and the recycle tank to overflow to a French drain if the water level rises above 3.2 m in either tank. The settling tank is also connected to the recycle tank just under mid depth (1.2 m) with a knife gate valve, allowing the two tanks to be used in conjunction if the settling feature is not required.

An 80 gpm submersible pump (Goulds WE1512HH) within the recycle tank delivers wastewater to the second stage cells. Wastewater drains from the second stage back to the recycle tank, with a portion of the flow diverted to a 6 m^3 tank (transfer tank). Flow to the transfer tank is regulated by a floating ball valve within the recycle tank. When the water level in the recycle tank is at 2.4 m or lower, all flow from the second stage enters the recycle tank. As the water level rises, the floating ball valve begins to close, sending a portion of the flow to the transfer tank and a portion back to the recycle tank. Once the water level rises to approximately 2.6 m, all flow from the second stage effluent is directed to the transfer tank. If the water level rises above 2.8 m, an overflow pipe sends water in the recycle tank to the transfer tank. Typically, the water level is at 2.4 m during the beginning of the cleaning cycle. The tank volume between this initial water level of 2.4 m and the overflow level of 2.8 m provides a buffer volume of 3.4 m^3. Provided the influent wastewater does not fill this buffer volume faster than the recycle tank pump doses the stage 2 cells, no overflow will occur and all flow entering the transfer tank will pass through stage 2, with no short circuiting of effluent from stage 1.

Two 40 gpm submersible pumps (Goulds WE0512HH) within the transfer tank then deliver wastewater to the third stage, the phosphorus adsorption beds. These pumps operate in a standard duplex mode, with an alternating lead and lag pump. The transfer tank is 1.5 m deep, and the lead pump turns on when the wastewater level in the transfer tank reaches 0.8 m. The lag pump will turn on if the lead pump cannot match the influent flow and the wastewater level rises to 0.9 m. Both pumps turn off when the wastewater drops to 0.5 m. The pump "on" and "off" levels are adjustable using the central control panel. Final effluent from the third stage flows by gravity through a 4-inch PVC pipe to either Blaine Springs Creek or to a small wetland area created for plant diversity and wildlife adjacent to the stream.

Stage 1 Wetland Design

The first stage is designed to receive vacuumed wastewater rich in solids to the wetland surface, accumulating a sludge layer by physically straining the suspended solids. This stage consists of five cells ("solids removal cells") operating in parallel, with motor actuated ball valves controlling which cell receives loading and whether the influent is sent directly to the solids removal cells or to the settling tank (Figure 4). Based on the criteria shown in Table 1, the first stage was designed with a total surface area of 150 m^2 (30 m^2 per cell). Cells were planted with *Schoenoplectus acutus* on August 13, 2015, and supplemented with additional planting in the summer of 2016 and on June 20, 2017 to fill in low density areas.

Each cell is lined with geotextile fabric, and contains the following from top to bottom: distribution piping, a treatment layer, a drainage layer, and drainage piping

(Figure 5). Wastewater is delivered to the surface of the solids removal cells through six 2-inch PVC pipes, rising vertically from the base of the wetland and terminating 53 centimeters above the wetland surface. This height allows solids to gradually accumulate and aerobically degrade on the surface of the treatment layer for many years prior to removal. The treatment layer consists of 0.46 meters of coarse media (d_{50} = 3.2 mm). The drainage layer consists of a 15 cm lower layer of coarse drain rock (d_{50} = 5-10 cm) surrounding the drainage piping, and an 8 cm upper layer of medium drain rock (d_{50} = 1 cm). A series of perforated 4-inch PVC drain pipe within the lower drainage layer collects wastewater after it has percolated through the treatment layer. The drainage piping consists of a center pipe with four lateral branches spaced every 1.2 m. The lateral branches are connected to non-perforated pipes extending above the surface of the wetland cells to provide an aeration pathway to the bottom of the wetlands. The central drain pipe is connected to a water level control structure, allowing for manual control of the water level within each cell.

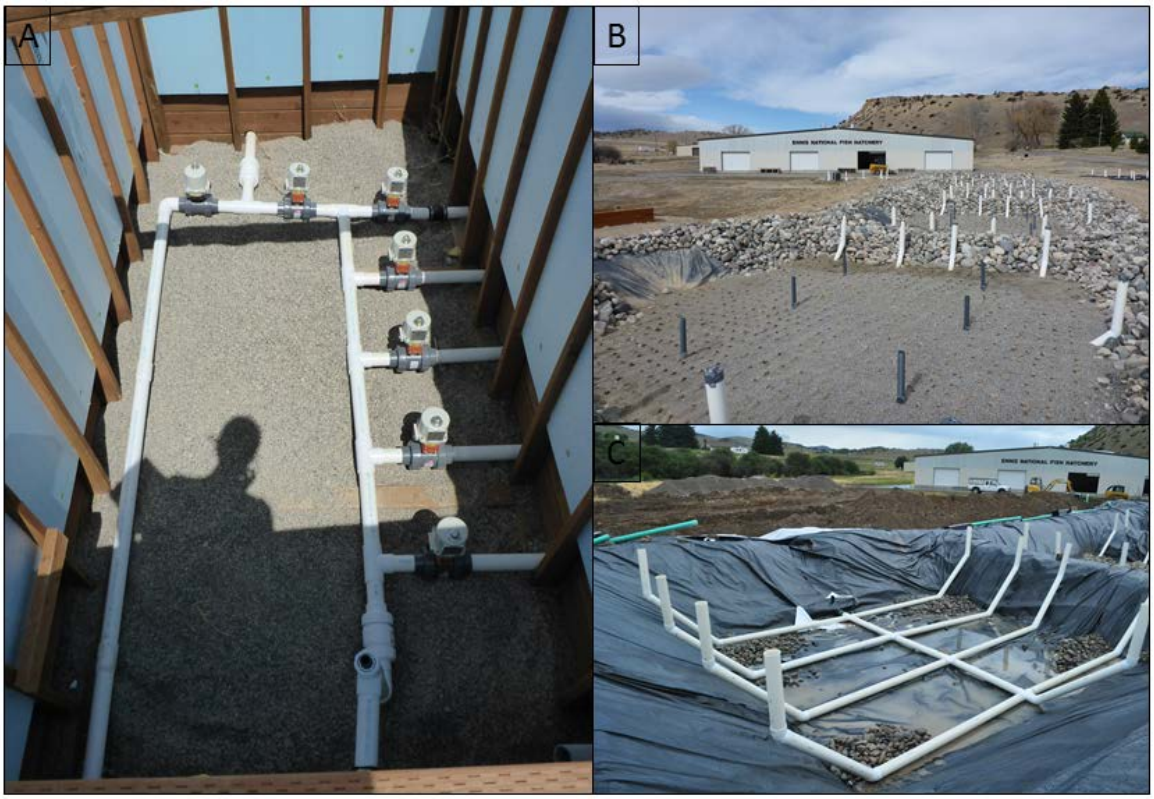


Figure 4. Stage 1 wetland cell valve distribution box (A), cells prior to plant establishment (B), and underdrain piping prior to fill with media. Vertical gray pipes in (B) are distribution lines, white pipes are vent pipes connected to drain lines.

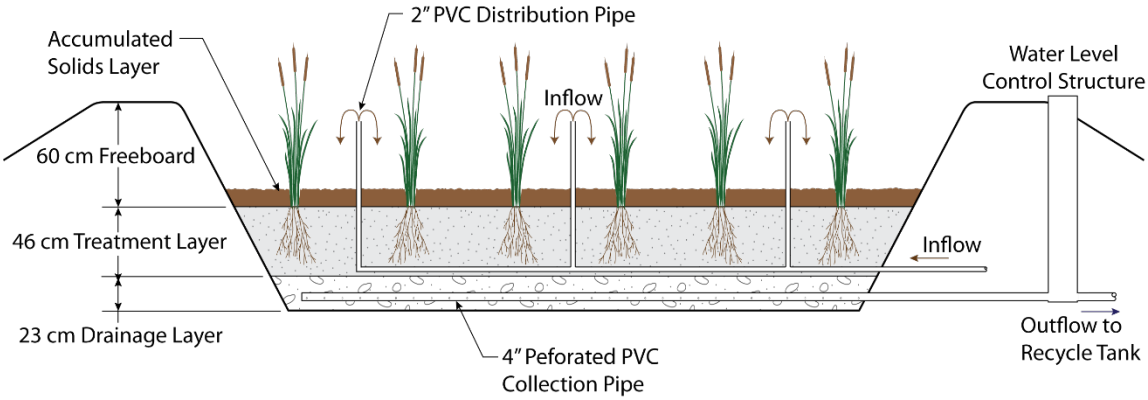


Figure 5. Stage 1 wetland cell cross section.

Stage 2 Wetland Design

The second stage is designed for biological removal of residual oxygen demand and dissolved nitrogen produced by the decomposition of solids in Stage 1. This stage consists of five cells ("nutrient removal cells") in parallel, with motor actuated valves controlling which cell receives loading, similar to stage 1. Based on the design criteria in Table 1, 67 – 168 m^2 is required for COD removal and 75 m^2 is required for nitrogen removal. A total surface area of 140 m^2 (28 m^2 per cell) was chosen to provide a conservative design and allow for flexibility in system optimization. Each cell was planted with a mixture of *Schoenoplectus acutus*, *Carex utriculata*, *Carex aquatilis,* and *Juncus arcticus* on August 13, 2015, and supplemented with additional planting on June 20, 2017 to fill in low density areas.

These cells are designed similarly to the solids removal cells, with the primary difference being a distribution pipe network lying above the treatment layer and below a protection layer (see Figure 6). The protection layer consists of 15 cm of coarse media (d_{50} = 3.2 mm), and serves as a thermal barrier against freezing for the distribution piping and to prevent human contact with wastewater. The treatment layer is slightly thicker than in the stage 1 cells, with 61 cm of coarse media (d_{50} = 3.2 mm). The drainage layer and drainage piping is identical to the stage 1 cells. The distribution piping consists of a 2-inch PVC main line in the center of the cell with 1 ¼–inch lateral branches at 50 cm intervals. The lateral lines are drilled with 8 mm orifices spaced every 36 cm to equalize flow distribution. Each lateral pipe terminates in a cleanout with a screw cap. Drainage

piping is similar to the solids removal cells, with a water level control structure for each cell and a common gravity sewer draining the stage 2 cells back to the recycle tank.

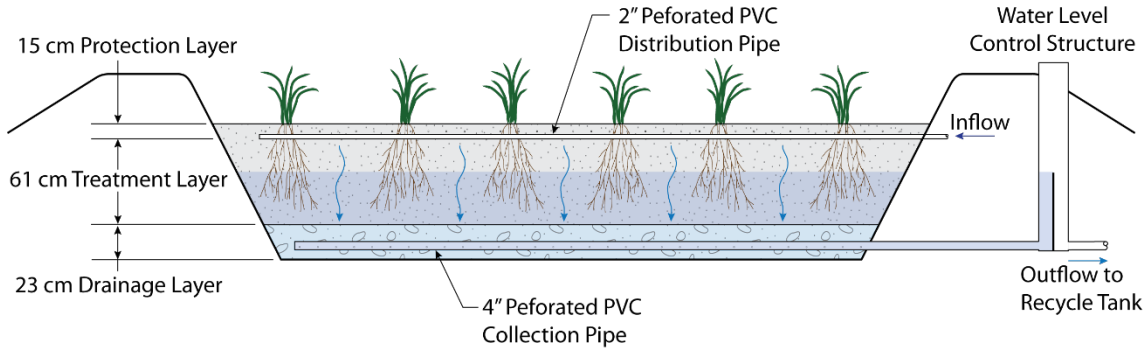


Figure 6. Stage 2 wetland cell cross section.



Figure 7. Nutrient removal cells prior to plant establishment. Vertical white pipes are vent lines connected to drainage piping.

Stage 3 Wetland Design

The third stage consists of three concrete horizontal flow cells, each 6.3 m^3 in volume and 0.61 m deep. With 0.15 m of freeboard each cell will hold 5.1 m^3 of media. The cells are currently empty, with the filter media to be chosen based on the results described in Chapter 3 of this thesis. Flow is split between these cells with an Orenco Hydrosplitter, which uses orifice discs to maintain equal head loss in each cell distribution pipe, ensuring near equal flow to each cell. Manually actuated ball valves can be used to further reduce or close flow to each cell.

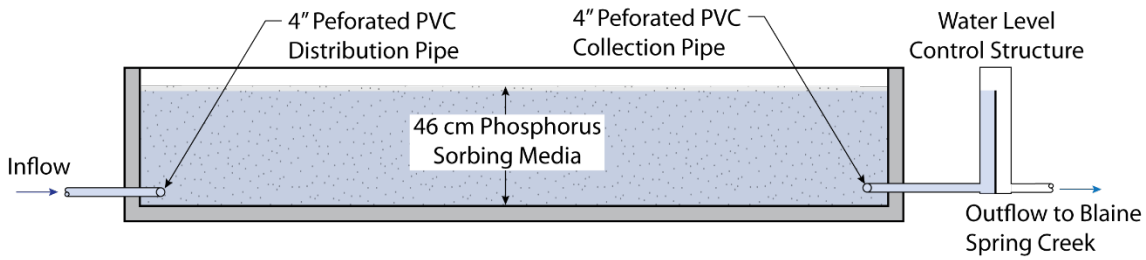


Figure 8. Stage 3 wetland cell cross section.



Figure 9. Phosphorus removal bed tanks prior to filling with media.

Control System

The system is controlled by a combination of manual and automated control parameters. An Allen-Bradley Micrologix 1400 programmable logic controller (PLC) controls the pumps in each tank and the actuated valves. The PLC is programmed with Allen Bradley RSLogix 500 software, and receives inputs from the influent flow meter, pump run times, float switches in each tank, a level sensor in the effluent tank, and pressure switches indicating when the collection system pumps are operating. By controlling the pumps and actuated valves, the PLC controls dose time, dose frequency, and which cell is dosed. These operating parameters can be set as constant values, or scaled based on feedback from the influent flow meter. A touchscreen operator interface terminal (OIT) allows the operator to change setpoints and observe flow rate, total flow, pump runtime, effluent tank level, pump and valve status, and alarms. Saturation levels in each cell can be changed manually using the water level control structures, and flow splitting between the third stage cells can be adjusted using ball valves.

Startup Operation and Sampling Methods

Operation

Construction of the first two wetland stages, including planting, was completed in autumn of 2015. The collection system was not functional at this point, with troubleshooting and refining of the system continuing through 2016. During this period, watering was infrequent and wetlands were kept semi-saturated to prevent plant death. Due to low growth in some wetland cells, additional planting was completed in the summer of 2016 and on June 20, 2017. Preliminary operation of the first stage began in

September 2016. Since pumps were not yet installed in any tanks, wastewater drained by gravity through each tank and to the emergency overflow French drain system. Design and installation of the control system was completed in March 2017, allowing the first two stages to operate as designed. To allow operation of the complete system, effluent from the second stage has been pumped directly to the Blaine Spring Creek until completion of the third stage, anticipated in August 2017.

Full scale operation of the first two wetland stages began on April 1, 2017. Vacuumed wastewater was sent directly to the first wetland stage, and the valve between the solids tank and recycle tank was opened, allowing for a larger effective volume of the recycle tank. After one week of operation, this valve was closed and the solids tank was pumped down to allow the solids tank to be used as a sampling location for influent wastewater, as discussed below. First stage effluent was directed to the recycle tank for distribution on the second stage.

During the first month of operation, the dose time and dose frequency of the nutrient removal cells was 3 minutes and 8 minutes, respectively, and this pattern cycled through all cells. Thus each cell was dosed for 3 minutes every 40 minutes. This resulted in a hydraulic loading rate (HLR) that was much higher than necessary, approximately 1.2 m d^{-1}. On May 10, the dose time and frequency were reduced to dose for 1 minute every 15 minutes (each cell dosed for 1 minute every 75 minutes), for an HLR of approximately 0.21 m d^{-1}. The nutrient cells were kept saturated to a depth of 0.3 – 0.6 m to encourage plant establishment during the first 2.5 months of operation, and fully

saturated to the wetland surface after the June 20th planting. The control panel recorded influent flow and pump run times, allowing for the calculation of HLR and recycle rates.

Sampling

Grab samples were taken from each tank by submerging a bottle in the tank and transferring to another bottle for storage. All samples were stored on ice in a cooler during transport to the lab. To obtain a representative influent sample, the solids removal tank was pumped down prior to raceway vacuuming, and vacuumed wastewater was subsequently sent to the empty solids removal tank. The contents of this tank was mixed while filling by using a small pump with a suction line pulling from one end of the tank and discharging through a 1-inch nozzle at the other end of the tank. This nozzle was attached to a handle allowing for movement to enhance mixing.

Influent wastewater samples were taken near the end of a cleaning cycle to maximize the sampling volume and best represent the average influent concentrations of a cleaning cycle. Recycle tank and effluent tank samples were taken after nearly all water in the solids removal tank had been applied to the first stage, so that it most closely represented water that had passed through the first stage cells and effluent tank sample represented water that had passed through the second stage cells with minimal recycle.

Water Quality Analysis

The pH was measured using an Accumet 13-620-AP50A pH electrode, either in the field directly after sampling or immediately upon return to the lab. Other constituents were measured either immediately or stored in a refrigerator at 4 °C prior to analysis. Samples for COD, total suspended solids (TSS), total Kjeldhal nitrogen (TKN), and total

phosphorus (TP) were not filtered prior to analysis. Samples for dissolved ions (ammonium, nitrate, nitrite, phosphate) were filtered with a 0.2 μm nylon syringe filter immediately upon return to the lab, prior to analysis. Reverse osmosis (18.2 MΩ) water was used for dilutions when required.

Several methods were used to determine water quality parameters. Chemical oxygen demand was analyzed using HACH Co. test kits following HACH Method 8000 (EPA Standard Method 5220D). Total nitrogen (TN) and TKN were analyzed simultaneously using HACH TNT880 kit (HACH Method 10242). Total phosphorus was measured using HACH Co. test kits following HACH Method 8190 for samples with concentrations below 10 mg L^{-1} (effluent tank and recycle tank) and HACH Method 10127 samples with concentrations above 10 mg L^{-1} (influent). Ammonium was determined using the 2-phenylphenol colorimetric method (Rhine et al., 1998). Nitrate, nitrite, and phosphate were analyzed using ion chromatography according to EPA Method 300.0 using a Thermo Scientific Dionex IonPac AS22-Fast 4x150 mm column. Organic nitrogen was determined by subtracting the ammonium concentration from the TKN concentration.

Results and Discussion

Hydraulic Loading

Daily wastewater production during full-scale operation is shown in Figure 10. Raceway cleaning occurred 2-3 days per week, typically in the middle of the workweek. This resulted in the stage 1 cells receiving 4-5 days of continuous rest between loadings, with the occasional one day rest between cleaning days. Cleaning volumes varied

between 3.0 – 24.5 m^3, with an average of 8.5 m^3. The average flow between May 1 and June 19 was 3.2 m^3 d^{-1}. Because actual cleaning volumes were lower than the assumed maximum volume of 18.9 m^3 and raceways were not cleaned 5 days per week, the actual average flow rate was much lower than the estimated average flow rate of 13.5 m^3 d^{-1}.

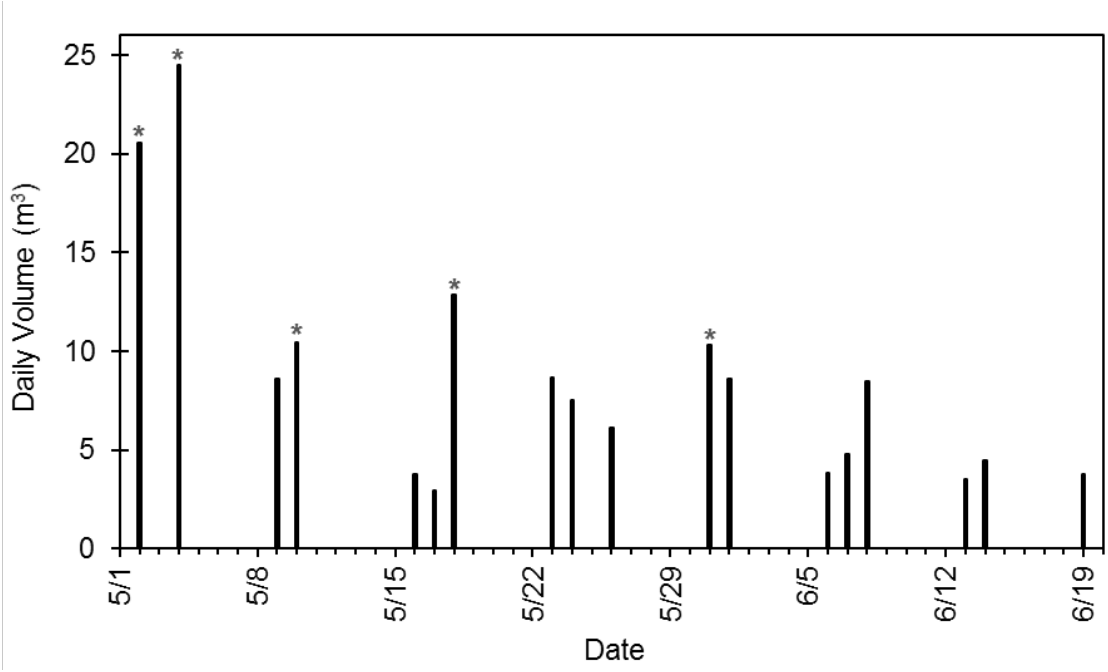


Figure 10. Daily cleaning volumes. Stars show days when grab samples were collected.

Pilot System Water Quality Results

Eighteen influent samples and twenty-two effluent samples were collected from the pilot system between August and October 2014 (Table 2). The pilot system removed 86% of COD, 90% of TSS, and 73% of TN. Samples were not analyzed for phosphorus or nitrogen species. A compost layer was added to the surface of two of the pilot system cells to improve solids filtering, but no difference was seen between effluent water quality before and after the compost layer was added.

Table 2. Pilot-scale wetland water quality results.

Parameter	Influent		Effluent		Units
	Average	SD	Average	SD	
COD	1672	485	229	88	mg L^{-1}
TSS	1107	582	114	14	mg L^{-1}
TN	43.2	17.7	11.8	2.5	mg L^{-1}

Full-Scale System Water Quality Results

Five samples were collected from each tank in the full-scale wetland in May 2017 (Table 3). Comparison of the influent and effluent shows the combined effect of the first two stages of the full-scale wetland which removed 98.5% of COD, 99.6% of TSS, 59.4% of TN, and 95.9% of TP.

Table 3. Full-scale wetland water quality results.

	Influent		Recycle Tank		Effluent Tank		
Parameter	Average	SD	Average	SD	Average	SD	Units
COD	2097.7	616.3	150.8	90.3	31.8	2.9	mg L^{-1}
TSS	1485.8	299.0	58.5	42.6	5.7	3.9	mg L^{-1}
pH	6.7	0.1	7.3	0.1	7.4	0.1	-
TN	78.7	23.1	39.6	8.9	31.9	16.2	mg L^{-1}
TKN	74.0	23.1	16.8	24.8	<0.5	-	mg L^{-1}
Org. N	67.1	18.8	14.5	24.3	<0.5	-	mg L^{-1}
NH_4-N	6.9	4.6	2.2	1.3	0.7	0.5	mg L^{-1}
NO_3-N	1.9	1.6	31.5	12.0	31.0	18.0	mg L^{-1}
NO_2-N	0.2	0.1	1.5	2.2	<0.5	-	mg L^{-1}
TP	48.4	11.5	6.3	1.5	2.0	0.7	mg L^{-1}
PO_4-P	7.0	1.9	3.3	1.0	2.3	0.5	mg L^{-1}

The influent COD, TSS, and TN was slightly higher in the full-scale system compared to the pilot system. This may be due to either differences in raceway cleaning operations, or differences in sampling procedures. Removal of COD and TSS improved significantly in the full-scale system compared to the pilot system, likely due to the

second stage and/or the slightly thicker treatment layer. Effluent COD, TSS, and TP concentrations also remained fairly stable in the full-scale system. It is important to note that data from both the pilot and full-scale systems was collected during a period of plant establishment and may not be representative of long-term performance.

The full-scale wetland had a lower nitrogen removal efficiency compared to the pilot system. However, effluent nitrogen concentrations decreased throughout this first month of data and removal efficiency at the end of the month was similar to the pilot system. Therefore it is likely that the observed differences are not significant. Nitrogen was present primarily in organic forms in the influent and as nitrate in the effluent.

The recycle tank contained primarily nitrate and organic nitrogen, with small amounts of ammonium and nitrite. The recycle tank samples are not a direct measure of the first stage effluent because that effluent is mixed with water that has passed through the second stage multiple times since the last cleaning. Thus samples from the recycle tank taken during an active cleaning cycle do not represent overall average concentrations, but rather maximum concentrations when wastewater is entering the system during cleaning. When no wastewater is entering the system, these concentrations are expected to decrease, as the wastewater is continuously recycled through the second stage. Nitrogen speciation in each tank is shown in Figure 11.

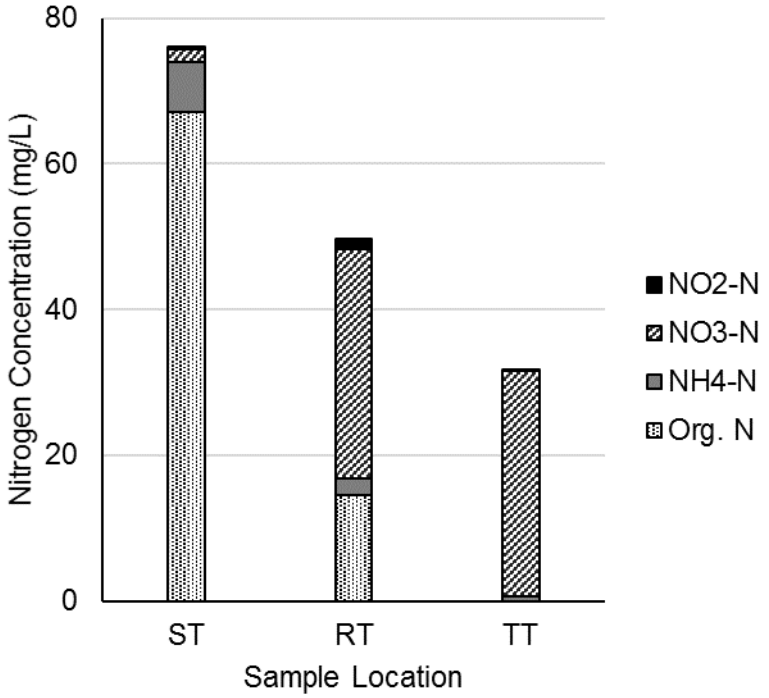


Figure 11. Average organic nitrogen, ammonia, nitrate, and nitrite concentrations in grab samples taken from the settling tank (ST), recycle tank (RT) and transfer tank (TT).

Comparisons of the influent and effluent nitrogen concentrations indicates ammonification of organic nitrogen and subsequent nitrification of ammonium within the two-stage system. One sample was collected directly from the stage 1 effluent rather than the recycle tank. This sample had nitrogen concentrations of 90.4 mg L^{-1} TKN, 18.2 mg L^{-1} Org.-N, 7.9 mg L^{-1} NH_4-N, 61.2 mg L^{-1} NO_3-N, and 4.9 mg L^{-1} NO_2-N. The first stage effluent had a higher total nitrogen concentration than the influent and the form was primarily nitrate. Nitrate fluxes in similar systems have been found to be irregular, with flushing of nitrate observed near the beginning of feeding periods and after resting periods (Pálfy et al., 2017; Silveira et al., 2015). In these systems, organic matter accumulated during feeding is thought to mineralize during resting periods creating

ammonium, and ammonium adsorbed on organic matter and wetland media is nitrified. During subsequent feeding periods, nitrate is desorbed from the organic matter and wetland media. A similar phenomenon is likely occurring in the first stage of this system, leading to the high nitrate concentration observed in the first stage effluent.

Influent phosphorus was composed primarily of organic or particulate P, although some orthophosphate was present. The first two stages removed all of the organic and particulate P (see Table 3 and Figure 12), with the effluent containing only orthophosphate (note that the water quality analysis showed more orthophosphate in the effluent than total phosphorus due to different methods used). The orthophosphate concentrations also decreased through the first two stages, indicating biological uptake and/or adsorption. The sample collected from the first stage effluent had 11.9 mg L^{-1} TP and 6.5 mg L^{-1} PO_4-P.

Unlike COD, TSS and TN which would be expected to decrease as plants become established and the system matures, total phosphorus will likely increase as sorption sites of the gravel media gradually saturate with orthophosphate. Plant and microbial uptake may mitigate this to a small degree, nevertheless mineralization of the sludge layer in the first stage will also produce additional orthophosphate. The concentration of phosphorus in influent of stage 2 can be estimated as between a lower bound of 7 mg L^{-1} (influent PO_4-P concentration), and an upper bound of 48 mg L^{-1} (influent TP concentration). Determining the timing and magnitude of PO_4 breakthrough from the first two stages is difficult, as it will depend upon mineralization, adsorption, and biomass uptake rates.

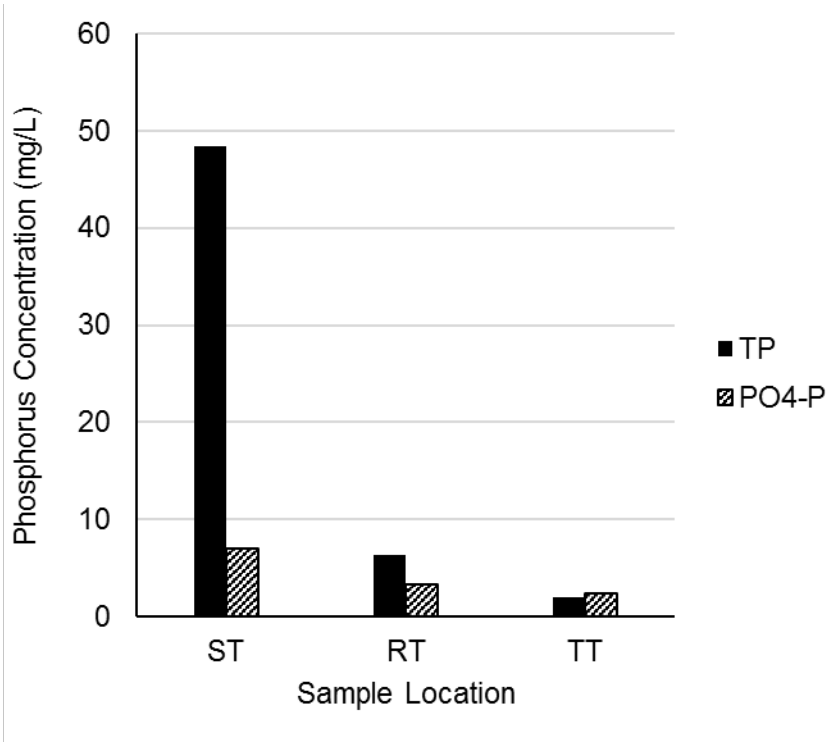


Figure 12. Average total phosphorus and orthophosphate in grab samples taken from the settling tank (ST), recycle tank (RT) and transfer tank (TT).

Flow meter and pump run time data were used to estimate the HLR and mass load, shown in Table 4. Currently, the first stage solids mass load is approximately 11.6 kg TSS yr^{-1}, significantly less than the design load of 50 kg TSS yr^{-1}. Due to small differences in elevation of the gravel surface within any stage 1 wetland cell, some short-circuiting occurs and the solids layer does not cover the entire wetland surface (see Figure 13). Surface loading of any particular point receiving solids is therefore much higher than the calculated average load. However, in the first year of operation, solids have begun filling in low spots, and surface loading is becoming more uniform.

The stage 2 mass loads were calculated based on concentrations measured from the single stage 1 effluent grab sample. The current COD mass load is significantly lower

than the design value, but the N mass load is very close to the design value. Stage 1 and stage 2 phosphorus loads were 1.0 and 0.3 g P m^{-2} d^{-1}, respectively (377 and 99 g P m^{-2} yr^{-1}). Because the stage 2 mass loads were calculated using only a single grab sample, they should be considered rough approximations. In particular, the nitrogen concentration in the stage 1 effluent will likely vary significantly, with flushing of nitrate expected to occur after resting periods as discussed above.

Table 4. Design parameters versus actual values for flow, HLR, stage 1 TSS load, stage 2 recycle rate, stage 2 COD load, and stage 2 TN load.

Parameter	Design Value	Actual Value	Unit
Average Daily Flow	13.5	3.2	m^3 d^{-1}
Stage 1 HLR	-	0.027	m d^{-1}
Stage 1 TSS Load	50	11.6	kg TSS yr^{-1}
Stage 2 HLR[1]	-	0.23	m d^{-1}
Stage 2 Recycle Ratio[1]	-	13	-
Stage 2 COD Load	40	10.3	g COD m^{-2} d^{-1}
Stage 2 TN Load	2.7	2.1	g TN m^{-2} d^{-1}

1. Stage 2 HLR and recycle rate after 5/10/17 dose time change.



Figure 13. Stage 1 wetland cell on May 10, 2017. Lighter regions on left and right sides show areas with no solids layer. Established plants are just breaking winter dormancy.

Contribution of Authors and Co-Authors

Manuscript in Chapter 3:

Author: Jack E. Wallis

Contributions: Generated experimental design, performed experiment set-up, data collection and analysis. Wrote the initial draft of the manuscript.

Co-Author: Otto R. Stein

Contributions: Assisted with experimental design and advised on data collection and analysis. Provided substantial edits on manuscript.

Co-Author: Christopher R. Allen

Contributions: Identified materials to test, advised on experiment set-up. Provided edits on manuscript.

Co-Author: Ellen G. Lauchnor

Contributions: Advised on experimental design, provided edits on manuscript.

Manuscript Information Page

Jack E. Wallis; O.R. Stein; C.R. Allen; E.G. Lauchnor

Water Science and Technology

Status of Manuscript:
_X_ Prepared for submission to a peer-reviewed journal
____ Officially submitted to a peer-review journal
____ Accepted by a peer-reviewed journal
____ Published in a peer-reviewed journal

SELECTING WETLAND MEDIA FOR PHOSPHORUS REMOVAL

Introduction

In the western mountain region of Montana, elevated phosphorus concentrations are found in many rivers and streams, threatening aquatic ecosystems. Although diffuse sources such as agricultural and urban runoff play a large role in high phosphorus levels, point sources such as wastewater effluent also discharge significant quantities of phosphorus and are more easily treated. Limiting phosphorus in wastewater effluent is therefore important to protect water quality from the negative ecological and human impacts of excessive P. Unfortunately, phosphorus is the most difficult nutrient to remove from wastewater because unlike nitrogen and carbon, the gas phase comprises only a small portion of the phosphorus cycle and phosphorus must therefore be removed as a solid phase.

The Ennis National Fish Hatchery is a large aquaculture facility located at the head of Blaine Spring Creek, a small tributary to the Madison River in southwest Montana. The hatchery diverts water from the springbox at the head of the creek, and water makes a single pass through the facility prior to discharge downstream. Due to the high flow rate through the hatchery, effluent typically contains low concentrations of contaminants. However, solids with high nutrient content settle onto raceway floors, and historically these solids were flushed to Blaine Spring Creek. Although these solids discharges were relatively infrequent, the high nutrient loads posed a threat to water quality. In response to growing concern over water quality and new regulatory requirements, the Ennis National Fish Hatchery recently constructed a three-stage

treatment wetland to treat solids rich wastewater generated by vacuuming solids from raceway floors. The first stage is designed to receive raw wastewater, physically straining solids on the wetland surface; the second stage is designed for biological carbon and nitrogen removal; and the third stage is designed for phosphorus removal.

Currently only the first two stages of the ENFH treatment wetland are operational, removing over 95% of influent phosphorus. However, effluent P concentrations are expected to rise as the adsorption capacity of the wetland media is saturated and the solids sequestered in stage 1 mineralize. To maintain high P removal, the third stage requires a filter media capable of adsorbing large quantities of phosphorus. The purpose of this study is to determine the optimal phosphorus removing filter material for the third stage. Six different locally available media were identified as potential filter media based on the results of a literature review. The adsorption capacities of these media were determined in batch adsorption experiments to compare the performance of each media. Different media particle sizes and water sources were tested to determine important parameters affecting phosphorus adsorption. Column tests were then conducted on the highest performing media to verify phosphorus removal capability under continuous loading conditions.

Literature review

Long-term phosphorus removal in treatment wetlands is difficult due to the nature of the phosphorus cycle. The phosphorus cycle consists of transformations between solid, aqueous, and gas phases, but unlike carbon and nitrogen, the gas phase comprises only a small portion of the phosphorus cycle (Glindemann et al., 2005). Because the solid phase

can be easily removed from wastewater via sedimentation and filtration, the challenge for phosphorus removal consists of transforming aqueous phases to a stable solid phase. Understanding phosphorus transformations in wetlands and the environmental factors that influence these transformations can therefore help in optimizing phosphorus removal in treatment wetlands. This literature review first examines the phosphorus cycle in wetland ecosystems. A detailed review phosphorus removal in SSF wetlands is then discussed, including removal mechanisms and successful filter media. The goal of this literature review is to assist in choosing a filter media for the ENFH treatment wetland that will provide long-term phosphorus removal.

Phosphorus Cycle

The phosphorus cycle in subsurface flow treatment wetlands consists of biotic and abiotic processes governing the transformation of phosphorus between various forms. In aquatic systems, a simplified partitioning scheme recognizes four forms of phosphorus: dissolved inorganic P (DIP), dissolved organic P (DOP), particulate inorganic P (PIP), and particulate organic P (POP) (Reddy et al., 1999). Dissolved inorganic phosphorus refers to the orthophosphate ion, PO_4^{3-}, and is also known as soluble reactive phosphorus (SRP). Particulate inorganic phosphorus is bound with calcium, iron, aluminum, or other elements, and can be classified based on the associated element (Reddy et al., 1999). Organic phosphorus (both dissolved and particulate) can be further classified as readily or slowly decomposable (Vymazal, 2007). Readily decomposable organic phosphorus includes nucleic acids, phospholipids, sugar phosphates, while more recalcitrant organic phosphorus includes inositol phosphates and phytin (Reddy et al., 1999). These more

complex fractionation schemes of organic and particulate inorganic forms can be quantified based using various laboratory extraction methods. In wetlands, P can be sequestered in macrophytes, microorganisms, wetland media, and sediments. These pools act as sources or sinks of phosphorus to the water, and mediate the transformation of phosphorus between different phases. A conceptual overview of the phosphorus cycle is shown in Figure 14.

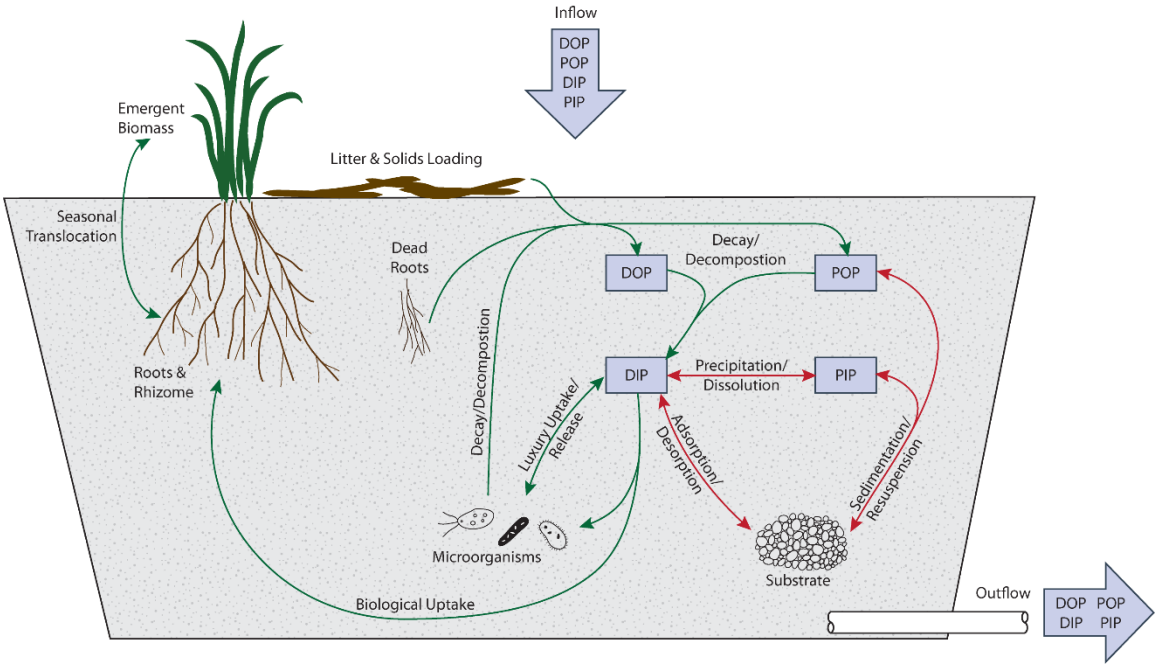


Figure 14. Phosphorus cycle in subsurface flow treatment wetlands. Green arrows indicate biological processes and red arrows indicate abiotic processes.

Plants act as both a sink and source of phosphorus, with the roots and rhizomes removing phosphorus directly from water, and dead biomass releasing phosphorus. Dissolved inorganic phosphorus is the only form known to be utilized directly by plants (Vymazal, 2007). Typically, the highest uptake rate occurs prior to maximum growth in early spring when plants store nutrients for later use (Reddy et al., 1999). During fall,

macrophytes translocate phosphorus from the shoots to the roots and rhizomes prior to senescence, allowing their use later during early spring growth (Reddy et al., 1999). Organic phosphorus in litter and dead roots can be released back into the water through abiotic leaching and biological decomposition (Vymazal, 2007).

Microorganisms uptake DIP directly from water, although the total amount of phosphorus stored in microbial biomass is typically small and quickly saturated (Kadlec & Wallace, 2009; Richardson, 1985). However, the microbial community is important in phosphorus cycling, serving as the first contact with influent phosphorus and capable of rapidly converting dissolved phosphorus to particulate forms (Kadlec & Wallace, 2009). Microbial communities are also important in decomposing litter and dead roots. Some investigators also suggest that microbial biofilms on the surface of wetland media can decrease adsorption, likely by limiting mass transfer to adsorption sites (Nilsson et al., 2013). Microorganisms may also influence water chemistry such as pH and redox conditions, altering phosphorus chemistry in the system (Reddy et al., 1999).

The wetland media is typically the greatest sink, sequestering phosphorus through both physical and chemical processes. Particulate forms of phosphorus can be removed through filtration and sedimentation within the wetland media, and soluble phosphorus can adsorb onto wetland media. Dissolved inorganic phosphorus can also precipitate directly from the water column if the chemistry is favorable. Adsorption is often the dominant process driving phosphorus removal in SSF treatment wetlands (Kadlec & Wallace, 2009; Vohla et al., 2011). However, adsorption tends to decrease with time as the media saturates with phosphorus.

Phosphorus Removal in Subsurface Flow Treatment Wetlands

Subsurface flow treatment wetlands typically have a low to moderate phosphorus removal capacity: in a review of 149 horizontal SSF and 78 vertical SSF wetlands, Vymazal (2007) found average phosphorus removal efficiencies of 41% and 60%, respectively. Because microorganisms represent only a small portion of the total phosphorus stored in treatment wetlands, the largest pools available for removing phosphorus are plants, sediments, and media. These are discussed further below.

Plant Uptake. Phosphorus stored in plant biomass can account for a substantial portion of influent phosphorus, with some systems designed for nutrient removal through biomass harvesting (Kadlec & Wallace, 2009). However, over 50% of plant biomass phosphorus is stored in the roots and rhizomes, limiting the amount of P capable of being harvested; aboveground biomass phosphorus has been reported in the range of 0.01–19 g m^{-2} (Vymazal, 2007). Because most SSF wetlands are loaded with 150 – 300 g m^{-2} yr^{-1}, biomass harvesting typically only removes low quantities of nutrients (Kadlec & Wallace, 2009). However, in lightly loaded systems biomass harvest may remove up to 40% of influent phosphorus (Kadlec & Wallace, 2009) and systems with higher loadings have been shown to remove substantial amounts of P. In an experimental scale three stage SSF wetland system, Vymazal and Kröpfelová (2011) found that aboveground biomass was responsible for removing 2.3-11.9% of the influent phosphorus (3.2–5.2 mg P L^{-1}) during the first two growing seasons. A mesocosm scale treatment wetland receiving waste activated sludge with 37 mg P L^{-1} was found to remove 6-17% of influent phosphorus during the second season of plant growth (Korboulewsky et al.,

2012). However, it is unclear whether the observed removal efficiencies were sustainable in these systems, or if the removal was due to increases in biomass during plant establishment.

Plant uptake has been shown to be important in short time scales. The uptake and release of phosphorus by plants creates a seasonal trend in effluent phosphorus concentrations, which can be seen in most horizontal SSF wetlands (Kadlec & Wallace, 2009). Concentrations are lowest during the early growing season as plants uptake phosphorus and higher after senescence and decomposition of litter. This can result in 100% removal during the growing season in lightly loaded systems such as grey water or polishing wetlands (Kadlec & Wallace, 2009). However, these seasonal trends tend to be small because in most treatment wetlands the total mass of phosphorus stored in plant biomass is low compared to the influent loadings.

Sedimentation and Filtration. Although sedimentation is typically avoided in subsurface flow treatment wetlands to avoid clogging, some systems are designed to physically filter solids from raw wastewater. The French style treatment wetlands are designed with a first stage receiving raw wastewater, physically straining solids and accumulating a sludge layer. In a survey of 20 French treatment wetlands receiving municipal wastewater, phosphorus removal averaged 45%, primarily within the first stage; in two wetlands receiving septage wastewater high in suspended solids, phosphorus removal averaged 94% (Paing & Voisin, 2005). Accumulation of solids was found to be a primary removal mechanism in these wetlands. In a pilot scale treatment

wetland receiving direct application of waste activated sludge, Korboulewsky et al. (2012) found that filtration of solids removed over 50% of influent phosphorus.

It is clear from these results that systems receiving raw wastewater can remove a significant portion of influent particulate phosphorus, particularly if the wastewater is rich in solids. However, phosphorus may also be released over time due to the mineralization of organic phosphorus within the sludge layer, often resulting in negative phosphorus removal after several years of operation (Paing et al., 2015). Physical filtration may therefore only be a short-term phosphorus removal mechanism, with more research needed to quantify long-term mineralization rates in sludge layers.

Adsorption. Adsorption of dissolved phosphorus onto wetland media is considered the primary removal mechanism in SSF wetlands (Kadlec & Wallace, 2009; Vohla et al., 2011). However, the adsorption capacity of wetland media is finite and typically saturates within years, depending upon mass loads and media characteristics (Vohla et al., 2011; Vymazal, 2007). Locally available sands and gravels are often used as wetland media, but generally exhibit low phosphorus adsorption capacity. In a review of treatment wetlands utilizing sand and gravel, phosphorus removal varied from -40% up to 54% removal, and typically decreased drastically after several months to years (Vohla et al., 2011).

To maintain long-term phosphorus removal, wetland media must be periodically replaced, which requires not only significant cost if planted cells are wholly removed, refilled, and replanted, but also infringes on the performance for other wastewater constituents. One option for overcoming this challenge is to use a separate stage designed

for easy removal and replacement of media (Arias et al., 2003; Vohla et al., 2011). Once phosphorus breakthrough occurs, saturated media can be removed from this separate cell without affecting treatment in the first stages. The disadvantage of this option is the initial cost associated with constructing a separate cell, as well as ongoing costs of removing and replacing adsorption media. To minimize these costs, considerable effort has been put towards finding media with high phosphorus adsorption capacity.

Many natural materials, manufactured products, and industrial byproducts have been identified as potential phosphorus sorbing wetland media. The majority of research has focused on calcium containing materials due to calcium's ability to bind with phosphorus, but magnesium, iron, and aluminum are also known to be important in some materials (Vohla et al., 2011). This review focuses on limestone, dolomite, shale, lightweight aggregate, and biochar, as these materials were found to be locally available in southwest Montana, and have shown promise for use as filter media. Biochar has not been extensively studied as a wetland media, but has received considerable attention for use as an agricultural soil amendment to reduce nutrient leaching, and shows promise as a phosphorus sorbent.

Filter media is often chosen based on adsorption capacities determined by lab scale batch experiments. Reported adsorption capacities for a given media can vary significantly between researchers, due to differences in source materials and experimental conditions (Cucarella & Renman, 2009). Phosphorus absorption by dolomite has been reported in the range of 121-51,000 mg P kg^{-1} (Vohla et al., 2011); limestone 250–20,000 mg P kg^{-1} (Vohla et al., 2011); sands and gravel 53–47500 mg P kg^{-1} (Vohla et al., 2011);

lightweight aggregates 37-12,000 mg P kg^{-1} (Vohla et al., 2011; Zhu et al., 1997); biochar 0–100,000 mg P kg^{-1} (Jung et al., 2015; Sarkhot et al., 2013; Yao et al., 2013); and shale from 384–954 mg P kg^{-1} (Drizo et al., 1999; Tang et al., 2009). It is important to note that although adsorption capacity is typically reported in terms of mass of P adsorbed per mass of adsorbent, density differences between materials must be considered when comparing materials for a full-scale application in which the volume may be fixed. In addition, although adsorption capacities determined by batch tests are useful for comparing different media performance under full-scale conditions can differ due to factors not taken into account (Cucarella & Renman, 2009). Examining the results of pilot- and full-scale systems is therefore necessary to determine the efficacy of different media.

Limestone has shown mixed success in full-scale systems. In a limestone filled wetland treating aquaculture wastewater, 92% of TP was removed over 1.5 years (Comeau et al., 2001). In an unplanted pilot scale filter bed filled with calcite ($CaCO_3$, the primary mineral in limestone), phosphorus concentration was reduced by 75%, from 5.7 mg/L to 1.4 mg/L (Arias et al., 2003). However, a limestone filled wetland receiving livestock yard runoff was only able to remove 4% of influent phosphorus over 1.5 years (Hill et al., 2000).

Prochaska and Zouboulis (2006) examined planted pilot scale systems with a mixture of sand and dolomite media over the startup period. Over the first month, phosphorus concentrations were reduced from 8 mg/L in the influent to less than 0.8

mg/L. Over the next two months, effluent phosphorus gradually increased to 4.1-4.4 mg/L, depending upon the loading, corresponding to 45-48.5% removal.

The performance of biochar can vary dramatically, depending upon feedstock and pyrolysis conditions (Sarkhot et al., 2013). In a series of planted wetland mesocosm experiments, adding biochar to sand actually decreased the phosphorus removal from 73% removal with no biochar to 52% removal with 25% biochar (de Rozari et al., 2016). In a comparison of 12 biochars produced from different feedstocks and pyrolysis conditions, only five were found to remove phosphorus in batch tests; the two with highest adsorption capacities were able to reduce phosphorus in column tests by 21% and 39% (Yao et al., 2012).

Many different lightweight aggregates (LWA) have been used in treatment wetlands, generally showing good performance. A treatment wetland filled with Filtralite, a LWA produced in Norway, removed more than 99% of phosphorus over the first three years of operation, with effluent P remaining below 0.2 mg L^{-1} (Heistad et al., 2006). The wetland was expected to meet the design lifespan of 5 years, estimated based on lab scale experiments. An Estonian LWA removed 89% of phosphorus from schoolhouse wastewater over two years (Öövel et al., 2007). Not all LWA's show such high performance, however. An expanded shale produced in Texas was only able to reduce phosphorus by 51% over 5 months, treating a low strength wastewater with influent SRP of 0.364–2.25 mg L^{-1} (Forbes et al., 2004). Another Norwegian LWA, Norlite, was only able to remove 34% of P over 1.5 years, treating livestock yard runoff (Hill et al., 2000)

Fewer literature reports have examined shale in full scale systems, but it shows considerable promise. A pilot scale wetland was able to remove 95–98% of phosphorus over 7 months, with high influent concentrations of 20–40 mg L^{-1} (Drizo et al., 2000).

Phosphorus Adsorption Mechanisms

Understanding adsorption mechanisms can assist in choosing media and operational strategies for maximum phosphorus adsorption. Phosphorus adsorption is a complex process, with the rate and magnitude dependent upon media physical and chemical properties, wastewater characteristics, and time (Cole et al., 1953; Vohla et al., 2011; Xu et al., 2014). Adsorption mechanisms have been well documented for calcium containing materials, but less information is available for biochar and iron and aluminum materials.

Many studies have examined adsorption mechanisms onto calcium containing materials such as limestone, apatite, dolomite, and calcite, due to availability and calcium's ability to bind with phosphate (Vohla et al., 2011). Although the term "adsorption" typically refers to a media's ability to remove phosphorus from solution, it is important to note that several distinct removal mechanisms have been identified, including physicochemical adsorption onto media surfaces, precipitation onto media surfaces, and growth of phosphate mineral crystals (Bellier et al., 2006; Cole et al., 1953; Johansson & Gustafsson, 2000; Xu et al., 2014). These mechanisms are closely related and difficult to observe independently, and therefore adsorption typically refers to the total effect of media on phosphorus removal.

Several investigators have observed three stages of phosphorus adsorption: adsorption onto surfaces, nucleation of phosphate mineral crystals, and growth of phosphate minerals by ongoing precipitation (Cole et al., 1953; Freeman & Rowell, 1981). At low phosphorus concentrations (up to 10-12 mg L^{-1} PO_4-P), phosphate adsorbed by calcite is readily exchangeable, indicating surface adsorption rather than precipitation of stable forms (Cole et al., 1953; Freeman & Rowell, 1981). As concentrations increase, exchangeable fractions decrease, suggesting precipitation of stable products. Surface adsorption models have also shown phosphate metal complexes forming on calcite and dolomite surfaces at low concentrations prior to the formation of calcium phosphate crystal phases (Xu et al., 2014).

As phosphorus concentrations increase, solid phases form on calcite surfaces. Nucleation is an important process affecting phosphorus removal, with increased adsorption rates observed when systems are seeded with metal-phosphate precipitates (Cole et al., 1953). Initial precipitates are typically different from the final equilibrium phase, with crystallization likely following the Ostwald-Gay Lussac Step Rule, which states that less thermodynamically stable and more soluble products are precipitated first (Zoltek, 1974). Calcium phosphate would therefore be expected to precipitate in the order of dicalcium phosphate ($CaHPO_4 \bullet 2H_2O$, DCP), tricalcium phosphate ($Ca_3(PO_4)_2$, TCP), octacalcium phosphate ($Ca_8H_2(PO_4)_6 \bullet 5H_2O$, OCP), and finally apatites (e.g. hydroxyapatite $Ca_5(PO_4)_3(OH)$). In experiments with calcite, Freeman and Rowell (1981) observed DCP formation on all samples with OCP on some samples using X-ray diffraction (XRD), which supported equilibrium models suggesting that phosphorus

initially precipitates as DCP and transforms to OCP over time. In batch experiments with calcite and dolomite, Xu et al. (2014) observed amorphous calcium phosphate ($Ca_3(PO_4)_2$, ACP), DCP, and hydroxyapatite (HAP) formation on surfaces at pH values from 6 to 8. Newberyite ($MgHPO_4$) was also observed on dolomite, although HAP was the primary phase found on both materials.

Many other calcium containing materials have shown evidence of a combination of adsorption and precipitation. Apatite itself has been studied as a phosphorus removal material, with the existing crystals thought to act as a catalyst lowering the activation energy required to precipitate phosphorus from solution (Bellier et al., 2006). In a pilot scale system with a calcium-rich hydrated oil shale ash filter, amorphous calcium and phosphorus containing precipitates were observed on particle surfaces with electron microscopy (Koiv et al., 2010). Total phosphorus removal rates showed a significant dependence upon loading rates, with removal increasing substantially when influent phosphorus was above 0.5 mg L^{-1} TP, indicating precipitation rather than surface adsorption processes.

Phosphorus adsorption by biochar is thought to be significantly different than mineral based sorbents. Several adsorption mechanisms have been identified, including exchange with surface hydroxyl groups, exchange with oxygenated functional groups, and hydrogen bonding (Chintala et al., 2014; Nelson et al., 2011; Sarkhot et al., 2013). Biochar may also have indirect effects on adsorption by changing water chemistry. Increased ionic strength may increase P sorption onto soils, and high base cation concentrations may provide larger positive surface charges to free divalent cations which

can precipitate P, such as Ca and Mg (Chintala et al., 2014). More research is needed to determine biochar adsorption mechanisms for different biochars and different wastewater characteristics.

Factors Influencing Phosphorus Adsorption

Phosphorus adsorption mechanisms are not well understood for all materials, and thus predicting how different material, environmental, or operational conditions may affect P removal is difficult. However, several factors are known to influence phosphorus adsorption including media composition, particle size, water chemistry, and certain operational strategies. Although the complex nature of adsorption makes predicting P removal in a given application difficult, these factors can help understand how phosphorus removal may change under different conditions.

Media Composition. In a review of phosphorus adsorbing filter materials, Vohla et al (2011) found that the calcium content of materials was roughly correlated with removal capacity, but the form of the calcium was a more important factor than the mere presence of the calcium element. Calcium oxide (CaO) and calcium hydroxide ($Ca(OH)_2$) were found to be much more effective at removing phosphorus than calcite ($CaCO_3$) due to the higher reactivity of these compounds. Some authors have suggested that high pH is associated with higher adsorption capacity (Cucarella & Renman, 2009), but others have noted that this higher adsorption can be explained by the high pH values associated with high CaO content (Vohla et al., 2011). Materials that had been heated often showed increases in phosphorus removal capacity due to the transformation of $CaCO_3$ to CaO (Vohla et al., 2011).

Composition is also important due to the ability to change pH conditions and release phosphorus binding metals such calcium. Some investigators have used different materials sequentially in a continuous flow reactor to take advantage of each materials unique properties. For instance, a layer of slag in the influent zone of a mixed apatite/limestone column filter enhanced the phosphorus removal compared to columns with mixed apatite/limestone/slag (Chazarenc et al., 2010). The slag layer raised the pH, creating more optimal precipitation conditions in the limestone/apatite zone downstream; the limestone was thought to release additional calcium, and the apatite provided nucleation sites for calcium-phosphate precipitate growth.

Particle Size. In a review of batch experiments on phosphorus adsorbing materials, Cucarella and Renman (2009) found that grain size was loosely correlated with removal capacity, with smaller grain sizes showing higher P removal. Studies comparing varying sizes of the same media have also shown significantly greater phosphorus removal by smaller sizes (Cyrus & Reddy, 2010; Li et al., 2013; Tang et al., 2009). The effect of size is mostly likely due to the larger surface area associated with smaller particles. This allows for greater dissolution of calcium per unit volume of media, increasing precipitation and crystallization of Ca-P phases (Vohla et al., 2011) and should also enhance other surface area dependent phosphorus removal processes such as adsorption.

Water Chemistry. Even with the same sorption media water with differing chemical signatures can have different phosphorus adsorption properties. Water of high ionic strength has been found to increase adsorption by Andisols (soils derived from

volcanic ash) with the type of electrolyte influencing P adsorption (Pardo et al., 1991). Water high in calcium ions performed best, followed by potassium and sodium (Pardo et al., 1991).

Water pH can have a complex and contradictory effect on phosphorus adsorption. In Andisols, increasing the pH from 3 to 7 decreased sorption, and increasing the pH from 7 to 9 increased sorption (Pardo et al., 1991). The decreasing adsorption as the pH increased between 3 to 7 was thought to be due to the decreasing net positive surface charge as the pH approached the point of zero charge (PZC), which was between 3.7-5.1, and the increasing net negative surface charge as the pH rose above the PZC. The increase in adsorption as the pH rose above 7 was attributed to the presence of phosphate primarily as HPO_4^{2-}, which may have had a greater affinity for soil particle surfaces than $H_2PO_4^-$.

Water pH may also affect dissolution and precipitation reactions. Calcite and dolomite have shown higher adsorption at pH values of 6 and 7 compared to pH of 8, which was attributed to the dissolution of calcium at the lower pH, resulting in the precipitation of calcium phosphates (Xu et al., 2014). Other researchers suggest that precipitation is favored by a high pH and high calcium to phosphorus ratio (Bellier et al., 2006). This would be expected if calcium phosphates are formed, as the solubility of these minerals decreases at high pH values (Figure 15). Iron and aluminum phosphates are less soluble at lower pH values, so if these metals are more available lower pH values may enhance precipitation.

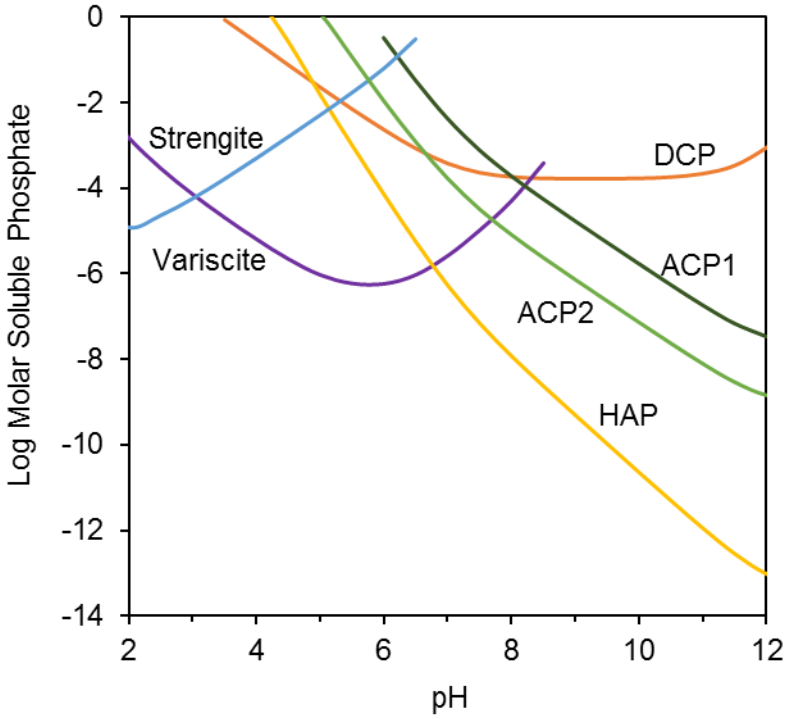


Figure 15. Solubility of strengite (iron phosphate), variscite (aluminum phosphate), DCP (dicalcium phosphate), ACP1 and ACP2 (amorphous calcium phophates), and HAP (hydroxyapatite). Modified from Stumm and Morgan (1996).

Redox potential is known to effect phosphorus removal by iron due to the difference in solubility between ferrous and ferric iron. At high redox potentials, iron oxidizes to ferric iron which can precipitate with phosphorus as ferric phosphate, or by precipitating as ferric hydroxide followed by adsorption of phosphate (Hill et al., 2000). Phosphate bound to ferric iron compounds may therefore be released if redox conditions transition from oxidized to reduced (Kadlec & Wallace, 2009).

Low molecular weight organic acids can decrease phosphorus adsorption through complexation of cations such as calcium, aluminum and iron which could otherwise precipitate phosphorus (Nelson et al., 2011). High BOD wastewater has also been shown to decrease phosphorus adsorption by some media, possibly due to biofilm growth

reducing mass transfer to media surfaces (Nilsson et al., 2013). However, not all media is affected by organic matter (Chazarenc et al., 2010). Adsorption onto biochar is also known to be significantly affected by the competition with other anions, especially sulfate (Sarkhot et al., 2013).

Operational Parameters. Hydraulic residence time (HRT) is the primary operational parameter affecting phosphorus removal. Phosphorus removal efficiency typically increases at longer HRTs (Cyrus & Reddy, 2010; Li et al., 2013; Tang et al., 2009). A wide range of residence times are used in pilot- and full-scale phosphorus filter beds, from as short as 0.22 days to as long as six weeks, with one to three days typical (Jenssen & Krogstad, 2003; Li et al., 2013; Nilsson et al., 2013). The optimal HRT depends upon the adsorption kinetics of the media. Cost may also influence the HRT chosen for a full-scale system, with filter bed size directly related to the residence time.

Resting filter media under drying conditions has also been shown to rejuvenate the phosphorus adsorption capacity of slag filter columns (Drizo et al., 2002). Drying conditions were thought to create localized areas supersaturated with calcium and other minerals, which would then precipitate forming new adsorption sites. However, in another study with a different slag, the resting of columns did not result in increased phosphorus removal (Chazarenc et al., 2010). This operational strategy therefore appears to show some promise, but may not be effective for all media.

Materials and Methods

Materials

Four natural materials and three manufactured materials were chosen for testing based on a literature review of successful phosphorus adsorbing materials and local availability. Natural materials included shale, limestone, dolomite, and gravel. Manufactured materials included a lightweight aggregate and two biochars processed from two different wood product materials.

The shale and limestone were sourced from a local landscape material supplier in Belgrade, Montana. The gravel and dolomite was sourced from an aggregate supplier in Ennis, Montana. The dolomite is a waste material from the Yellowstone Mine, a talc mine located in Cameron, Montana. The gravel is a fractured chip seal aggregate, and is the same material used as the treatment layer in the treatment wetland system.

The lightweight aggregate (Utelite) is an expanded shale material produced by Utelite Corporation in Salt Lake City, Utah. Utelite is produced from a shale of the Frontier Formation in a rotary kiln at a temperature of approximately 1100 °F. The two biochars were produced from juniper and lodgepole pine. The juniper biochar was produced by a partnership between the University of Utah and Amaron Energy using feedstock from land clearing operations in a mobile rotary pyrolysis kiln. The lodgepole pine biochar was produced by Confluence Energy with beetle killed lodgepole pine feedstock.

The shale, limestone, and dolomite materials were crushed to a size which would be used in the filter beds. All materials were sieved and separated into 0.841 – 2.00 mm

("fine") and 2.00 – 4.76 mm ("coarse") size fractions, corresponding to material retained on a #20 and #10 standard sieve. Each sieved material was then rinsed in tap water to remove dust. Mineral materials (shale, limestone, dolomite, gravel and lightweight aggregate) were air dried for a minimum of 48 hours prior to testing. Due to its high water retention capacity, biochar was oven dried at 150 °C for a minimum of 24 hours prior to testing.

Elemental composition of all materials except biochar was determined by X-ray fluorescence (XRF) with a ThermoFisher Niton XL3t GOLDD+ analyzer. Biochar was not analyzed using XRF due to the interference of organic carbon on results.

To determine the pH of each material, a measured quantity of each material was equilibrated in 10 mL of Blaine Spring Creek water and deionized water for 24 hours. The pH of gravel, dolomite, shale, limestone, and Utelite was found using 10 g of material. Due to its significantly lower density, only 2.5 g of biochar was used to provide a similar solid volume to liquid volume ratio.

Batch Adsorption Tests

Batch tests were conducted following OECD test 106 guidelines (OECD, 2000). Phosphorus solutions were made using monobasic potassium phosphate (KH_2PO_4) and dibasic potassium phosphate (K_2HPO_4) in a ratio of 1:2.7, resulting in a pH of approximately 7.5. Media was equilibrated in phosphorus solutions of varying initial concentrations and adsorbed phosphorus was calculated based on the difference between the initial and final concentrations after 24 hours of equilibration. In all tests, the pH was measured just after adding the phosphorus solution and after 24 hours of equilibration.

The media to solution ratio was determined in a series of preliminary batch tests at varying ratios using an initial P concentration of 10 mg L^{-1}. The eventual ratio was chosen so that approximately 20 – 50% of the phosphorus in solution would be adsorbed and was unique for each media type and size in subsequent batch tests (Table 5). Three replicate batch experiments were completed at eight initial phosphorus concentrations (0, 5, 10, 20, 40, 80, 160, and 320 mg L^{-1}) and using deionized water and Blaine Spring Creek (BSC) water.

Table 5. Media to solution ratios for each media in adsorption isotherm experiments.

Media	Media Size (mm)	Media Mass (g)	Solution Volume (mL)	Media:Solution Ratio (g:g)
Gravel	2.00 – 4.76	50	50	1:1
Dolomite	2.00 – 4.76	50	50	1:1
Limestone	2.00 – 4.76	50	50	1:1
Limestone	0.841 – 2.00	25	50	1:2
Shale	2.00 – 4.76	50	50	1:1
Shale	0.841 – 2.00	25	50	1:2
Utelite	2.00 – 4.76	8	100	1:12.5
Utelite	0.841 – 2.00	2	100	1:50
Lodgepole Biochar	2.00 – 4.76	2.5	50	1:20
Juniper Biochar	2.00 – 4.76	2.5	100	1:40

Batch tests in phosphorus solutions made with deionized water were conducted for Utelite (fine and coarse), limestone (fine and coarse), shale (fine and coarse), dolomite (coarse), and gravel (coarse). Stock solutions of 80, 160, and 320 mg L^{-1} phosphorus were made and stored in a refrigerator. These stock solutions were then diluted as necessary and added to 200 mL Erlenmeyer flasks containing measured quantities of media. Water samples were taken before the diluted solution was added and

after 24 hours of equilibration and analyzed for orthophosphate. Three blanks containing no media at each concentration was included in each test.

Batch tests in phosphorus solutions in BSC water were conducted for coarse Utelite, limestone, shale, gravel, and biochar. For these tests, 800, 1800, and 3600 mg L^{-1} P stock solutions were made in deionized water. Small volumes of each were then added to 200 mL Erlenmeyer flasks containing measured quantities of media and BSC water to result in the specified initial concentrations. Samples were taken after 24 hours of equilibration. Blanks were also made with deionized water using this method to verify initial concentrations. Because some phosphorus was expected to precipitate with the calcium in the BSC water, the initial concentration was not sampled and analyzed. Three blanks with BSC water containing no media at each concentration were also tested to determine how much phosphorus would precipitate with the BSC water.

The mass of adsorbed phosphorus per mass of media was calculated based on the change in concentration after 24 hours of equilibration according to equation 1:

$$q = \frac{(C_i - C_e)V}{M} \qquad \text{(eq. 1)}$$

q = Mass of phosphorus adsorbed per mass of media [mg kg^{-1}]

C_i = Initial concentration [mg P L^{-1}]

C_e = Equilibrium concentration [mg P L^{-1}]

V = Solution volume [L]

M = Mass of media [kg]

Data analysis utilized Microsoft Excel software. Two adsorption models were fit to the batch isotherm data: the Langmuir and Freundlich isotherm equations, shown as equations 2 and 3, respectively:

$$q = \frac{q_0 K_L C_e}{1 + C_e K_L} \quad \text{(eq. 2)}$$

q_0 = Maximum adsorption capacity [mg kg^{-1}]

K_L = Binding strength constant [mg P L^{-1}]

$$q = K C_e^{1/n} \quad \text{(eq. 3)}$$

K = Adsorption capacity at unit concentration [(mg kg^{-1})(L mg^{-1})$^{1/n}$]

n = Binding strength constant [dimensionless]

Nonlinear regression using the Generalized Reduced Gradient (GRG) algorithm was used to fit the Langmuir and Freundlich equations to the isotherm data using the maximum likelihood estimate (MLE) method (Brown, 2001; Scholz, 2004).

Column Tests

Continuous flow tests were performed in vertical up-flow columns constructed of nominal 2-inch schedule 40 PVC pipe (inside diameter 5.25 cm) with a total filled length of 35 cm and volume of 0.75 L. Gravel, Utelite, and lodgepole biochar media were tested. The gravel columns contained 1120 g of coarse gravel. Two column configurations were tested with Utelite, both with significant quantities of gravel added to prevent excessive pH increases in the column effluent. The “layered” column consisted of three layers,

from bottom to top: 150 g gravel, 100 g Utelite, and 800 g gravel. The “mixed” column also consisted of three layers: 150 g gravel, 100 g Utelite mixed with 800 g of gravel, and 20 g of gravel. The lodgepole biochar column consisted of 100 g of biochar sandwiched between two 150 g gravel layers. To provide a more realistic estimate of how much P would be removed in a field scale system, the Utelite and lodgepole biochar were not separated into coarse or fine size fractions, but used at the gradation supplied from the source. The gradations used had much more fine particles than the sieved materials, and only slightly more coarse particles. Three replicates of each column configuration shown in Figure 16 were tested.

Columns were fed using two multichannel peristaltic pumps, with suction tubing placed in one of two feed containers. The flow rate was initially set to result in a hydraulic retention time (HRT) of approximately 24 hours. To shorten the experiment time, the HRT in the Utelite columns was decreased to approximately 12 hours after several weeks of operation. The HRT was calculated based on the measured pore volume and flow rate. The pore volume was measured at the start of each experiment by filling each column from a graduated cylinder with a peristaltic pump and measuring the quantity of water required to fill each column. The quantity of water drained from each column immediately after filling was also measured to determine the “wetted volume”, or the hydroscopic volume retained after gravity draining. The flow rate was measured at the start of each experiment and periodically throughout the experiment by closing the influent valve and measuring the quantity of water out of the flow measurement port over a period of 1–3 hours (see Figure 16). The flow rate tended to decrease gradually with

time and was adjusted to the design flow several times throughout the duration of the experiment.

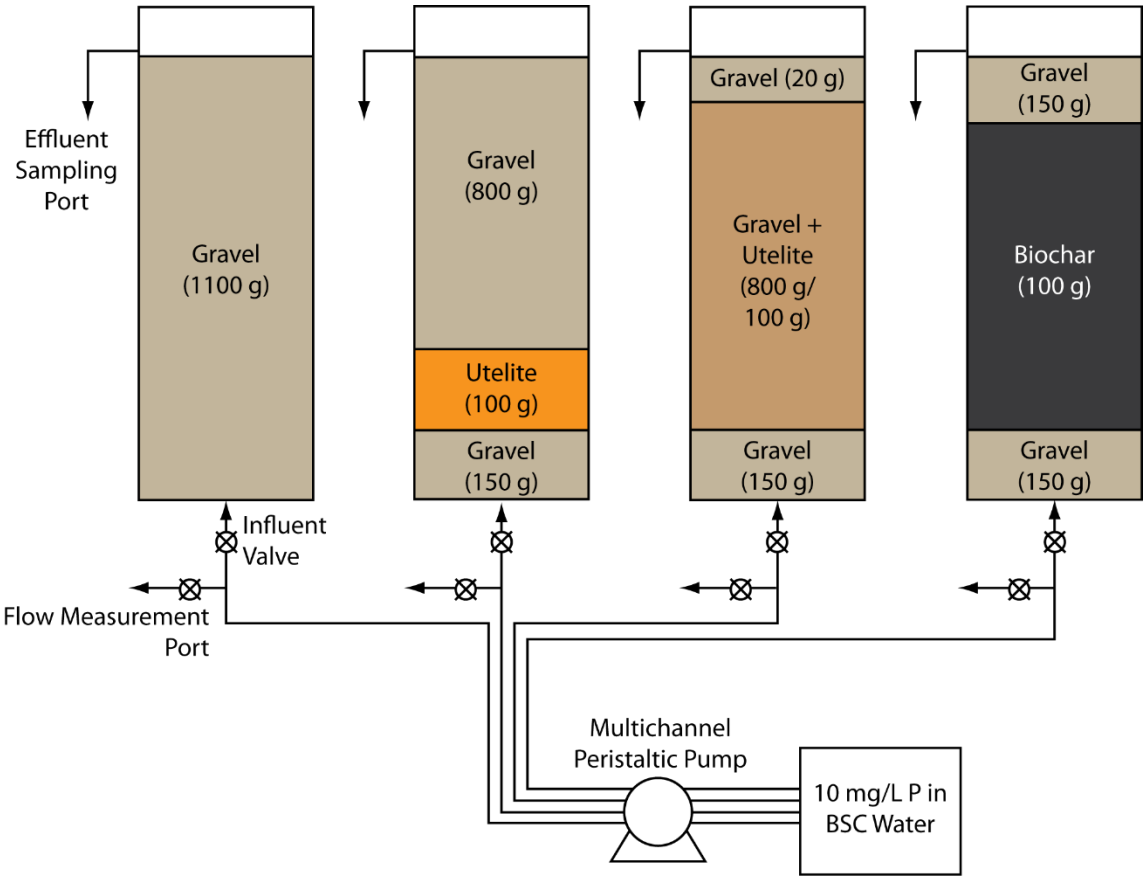


Figure 16. Configuration of column experiments.

Samples were taken from the feed containers and the column effluent sampling port typically once per day and the pH of each sample was measured. Approximately 1 hour was required to obtain a 15 mL effluent sample, and the sample concentration was assumed to be representative of the effluent concentration at middle of the sampling period. The flow rate at each sampling time was determined by assuming the flow rate decreased linearly between flow measurements. The flow rate, feed concentration, and

effluent concentration were then used to calculate total P loading and total P removal by using trapezoidal integration between sampling times.

To determine the amount of phosphorus adsorbed by the Utelite and biochar exclusive of the gravel, a logarithmic trendline was fitted to a plot of phosphorus adsorption by the gravel columns versus the number of pore volumes that passed through the column. The equation of this trendline was then used to estimate the quantity of phosphorus adsorbed by the gravel in the Utelite and biochar columns, and this quantity was subtracted from the total adsorbed phosphorus to estimate the amount of phosphorus removed by the Utelite or biochar alone.

During the transition between the 24-hour and 12-hour residence time tests, the flow was halted for several days while the Utelite columns were full. Concentration data before, during, and after this transition was used to determine the effect of residence time on removal efficiency by plotting the removal efficiency versus hydraulic residence time assuming ideal plug flow. The k-C* modified first order rate equation (Kadlec & Wallace, 2009) shown as equation 4 was then fit to this data:

$$\frac{C - C^*}{C_0 - C^*} = e^{-kt} \qquad \text{(eq. 4)}$$

C = Effluent concentration [mg L^{-1}]

C_0 = Influent concentration [mg L^{-1}]

k = Reaction rate constant [d^{-1}]

t = Hydraulic residence time [d]

Water Quality Analysis

The pH was measured using an Accumet 13-620-AP50A pH electrode. All samples were filtered with a 0.2 μm nylon syringe filter prior to analysis of dissolved ions. Samples were either analyzed immediately after filtration or stored in polyethylene centrifuge tubes at 4 °C. Dissolved ions were analyzed using ion chromatography according to EPA Method 300.0. Orthophosphate was analyzed using a Thermo Scientific Dionex IonPac AS22-Fast 4x150 mm column. Due to the close proximity of sulfate and phosphate peaks using this column, samples high in sulfate taken during the initial operation of Utelite columns were analyzed using two AS22-Fast columns in series. This resulted in sufficient separation of phosphate and sulfate peaks for quantification. The detection limit was considered the lowest concentration at which the standard curve was able to accurately predict check standards of known concentration; this was 0.5 mg L^{-1} PO_4-P.

Statistical Analysis

Comparisons between mean values of batch adsorption results at each concentration were completed using the two-way analysis of variance (ANOVA) method with 95% confidence interval and Tukey's test. Comparisons of all other mean values was completed using the one-way ANOVA method, also with a 95% confidence interval and Tukey's test. Results were considered significant if the p value was less than 0.05.

Results

To screen for suitability as a phosphorus adsorbing filter media, materials were characterized by composition, pH, and phosphorus adsorption capacity under batch conditions. Batch tests were completed with coarse media in DI water, fine media in DI water, and coarse media in BSC water to determine important parameters affecting P adsorption. Two of the top performing media (Utelite and lodgepole biochar) were then tested for P removal capacity under continuous flow conditions along with gravel to provide a baseline comparison.

Media Characteristics

All materials except the biochars were characterized by elemental composition using XRF analysis, shown in Table 6. Biochar was not tested due to the interference of organic carbon preventing accurate results. The composition of the media varied, particularly in Ca content. The Utelite and gravel had the most similar compositions, with moderate amounts of calcium and iron, and lower levels of magnesium, aluminum, and P. The shale was similar in composition for most elements, but with much less calcium. The limestone and dolomite were similar to each other, with larger amounts of calcium, especially the limestone, than the other materials, and no phosphorus was detected in either. The dolomite had more iron and silicon than limestone but less magnesium despite that being a characteristic of dolomite.

Table 6. Elemental composition of mineral media.

	Elemental Composition (% wt)					
Material	Ca	Mg	Fe	Al	Si	P
Gravel	3.39	0.22	2.38	0.64	11.30	0.06
Utelite	4.88	0.38	3.12	1.06	10.79	0.05
Shale	0.19	0.19	2.75	1.08	12.14	0.07
Limestone	44.08	0.77	0.03	0.20	0.49	nd[1]
Dolomite	11.94	0.39	1.85	0.20	1.80	nd[1]

1. nd = no detection

The pH of 10 mL solutions of DI and BSC water containing 10 g of the mineral materials and 1.5 g of biochar generally varied between 8 and 9, except for fine Utelite and juniper biochar which were above 9 (Table 7). Blanks consisting of 10 mL of DI water and BSC water without media had pH values of 7.9 and 8.4, respectively. However, the accuracy of pH readings in the DI water blank are questionable, as the theoretical pH should be near 7; pH sensors are known to give poor readings in waters with low ionic strength, which may be the source of this discrepancy. Fine and coarse Utelite and coarse limestone significantly increased the pH of DI water compared to the DI blank. The remaining materials increased the pH of DI water compared to the blank, but this effect was not significant.

Utelite, juniper biochar, and lodgepole biochar significantly increased the pH of BSC water compared to the blank, while limestone and shale significantly decreased the pH. Gravel and dolomite had no effect on the pH of BSC water. The pH of Utelite, gravel, and dolomite in BSC water was higher than the same materials in DI water, which was expected as the BSC water had a higher pH than the DI water. The opposite effect was observed for limestone and shale, with lower pH values in BSC water than in DI water.

Table 7. pH of media in DI and BSC water.

Material	Size Fraction	pH in DI Water	pH in BSC Water
Utelite	Fine	9.3	10.1
	Coarse	8.6	8.6
Limestone	Fine	8.4	8.1
	Coarse	8.5	8.1
Shale	Fine	8.3	8.0
	Coarse	8.2	8.2
Gravel	Coarse	8.1	8.4
Dolomite	Coarse	8.3	8.4
Juniper Biochar	Coarse	-	9.2
Lodgepole Biochar	Coarse	-	8.8
Blank	-	7.9	8.4

Batch Adsorption Isotherms

Adsorption capacity of each media was determined from batch experiments at initial phosphorus concentrations ranging from 0 – 320 mg L^{-1}. Gravel, dolomite, limestone, shale, and Utelite were tested with coarse (2.00 – 4.76 mm) particle sizes, and limestone, shale, and Utelite were also tested with fine (0.841 – 2.00 mm) particle sizes, all in DI water. Gravel, limestone, shale, Utelite, juniper biochar, and lodgepole biochar were also tested with coarse particles in BSC water. Results of batch isotherm experiments of coarse media in deionized (DI) water are shown in Figure 17. The adsorption capacity of Utelite was significantly greater than all other media at P concentrations above 5 mg L^{-1} ($p<0.05$), and Utelite was the only media to adsorb substantial amounts of phosphorus at concentrations below 80 mg L^{-1}. Limestone had the next highest adsorption capacity at concentrations above 80 mg L^{-1}, followed by shale, gravel, and dolomite respectively. However, the differences between shale, gravel, and dolomite were not statistically significant. At concentrations below approximately 50 mg

L^{-1}, shale had a higher adsorption capacity than limestone, although this effect was not significant.

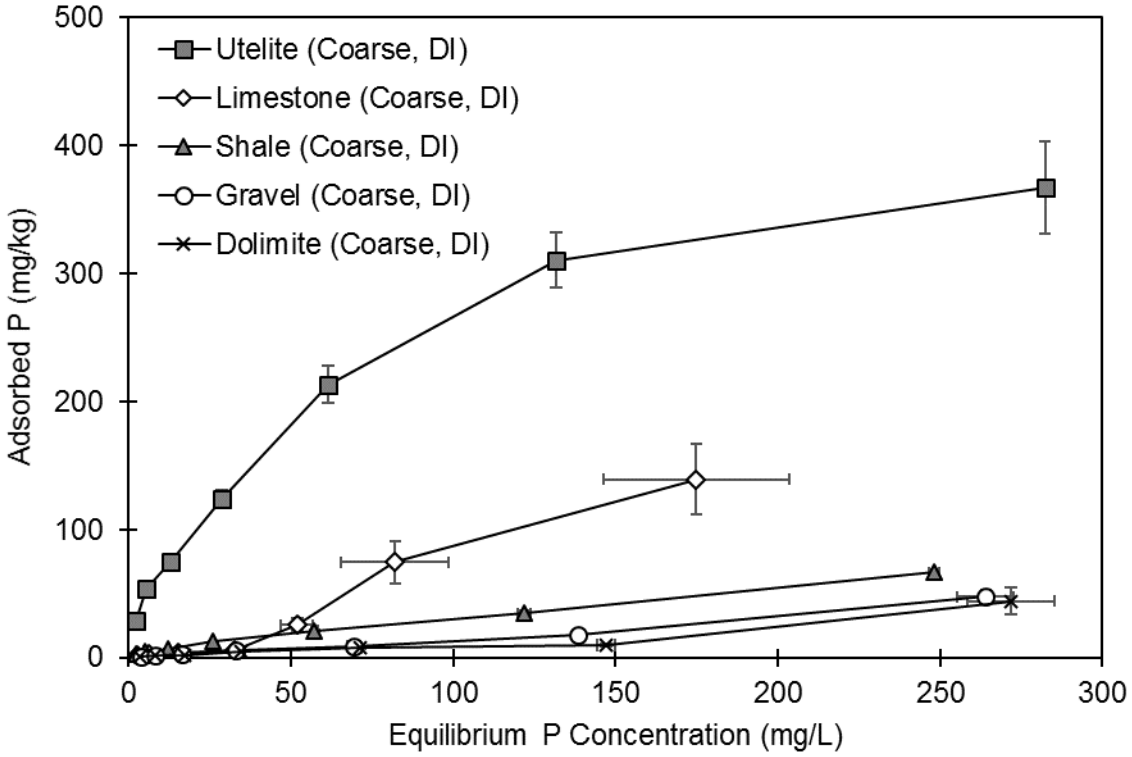


Figure 17. Adsorbed P versus equilibrium aqueous P concentration of all coarse size fraction media tested in DI water. Error bars represent standard error (n=3).

Results of batch isotherm experiments of coarse media in BSC water are shown in Figure 18. The general shape of the isotherms and ranking of mineral materials was similar as in DI water but Utelite had a higher adsorption capacity and limestone had lower capacity in BSC water. The biochars generally performed better than the mineral materials except Utelite but with a unique isotherm shape. As a result, at concentrations above 10 mg L^{-1}, Utelite, juniper biochar, and lodgepole biochar adsorbed significantly more P than shale, gravel, and limestone. Between 5 and 80 mg L^{-1}, juniper biochar adsorbed significantly more P than Utelite, but at higher concentrations Utelite adsorbed

more. Lodgepole biochar performed similarly to Utelite at concentrations between 5 and 40 mg L^{-1}, but adsorbed significantly less at higher concentrations. Juniper biochar adsorbed significantly more P than lodgepole biochar at all concentrations. Of the remaining materials, shale had the highest adsorption capacity, followed by gravel and limestone, although the differences between these materials was not statistically significant.

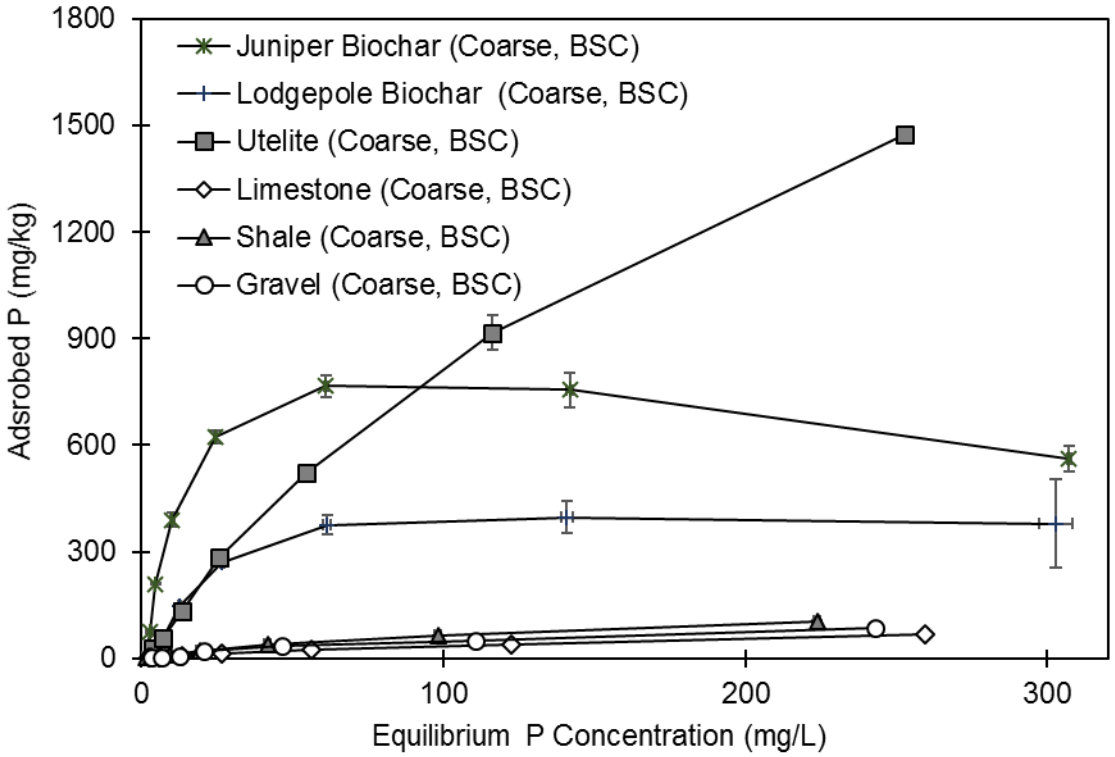


Figure 18. Adsorbed P versus equilibrium aqueous P concentration of all coarse size fraction media tested in BSC water. Error bars represent standard error (n=3).

Utelite, limestone, and shale were tested with fine particles (0.841 – 4.76 mm) in DI water to determine the effect of particle size on phosphorus removal. The fine Utelite and limestone particles adsorbed more P than coarse particles in DI water, while the fine

shale was not substantially different at the two sizes. The effect of size for each material is discussed further below.

Adsorption Isotherm Equations. The isotherm data from both the DI and BSC experiments was fit to Langmuir and Freundlich isotherm equations (equations 2 and 3), summarized in Table 8. In general, both equations fit the data well with high coefficients of determination (r^2). The Langmuir isotherm tended to fit the data better than the Freundlich isotherm, and it is the only isotherm shown on the plots below. However, the difference in fit between the two isotherm equations was typically small.

The adsorption capacity of some materials appeared to reach a maximum value at low equilibrium concentrations, followed by a steep increase in adsorption capacity as the concentration increased past an inflection point. This inflection point is not present in the Langmuir or Freundlich isotherm equation, and may indicate a transition from physico-chemical adsorption to precipitation processes (Cole et al., 1953). In these cases, the isotherm equation was fit to only the portion of the data prior to the inflection point. This range was 0-40 mg L^{-1} for fine Utelite in DI water, and fine and coarse limestone in DI water; 0-80 mg L^{-1} for Ennis gravel; and 0-160 mg L^{-1} for dolomite. Therefore, despite the high coefficients of determination for these materials, neither the Langmuir nor the Freundlich isotherm can be considered a good model over the full range of concentrations measured.

Table 8. Maximum adsorption capacity, Langmuir, and Freundlich coefficients.

Substrate	Max.	Langmuir			Freundlich		
	q ($mg\ kg^{-1}$)	q_0 ($mg\ kg^{-1}$)	K_L ($L\ mg^{-1}$)	r^2	n	K_f (2)	r^2
Coarse Media in DI Water							
Utelite	367.1	457.8	0.015	0.95	0.46	28.8	0.93
Limestone[1]	174.9	6.7	0.16	0.86	0.38	1.6	0.94
Shale	66.5	202.2	0.0019	0.98	0.77	0.93	0.98
Ennis Gravel[1]	47.7	16.1	0.016	0.62	0.69	0.47	0.60
Dolomite[1]	44.3	15.0	0.014	0.89	0.57	0.59	0.87
Fine Media in DI Water							
Utelite[1]	1189.2	298.8	2.6	0.88	0.10	219.2	0.87
Limestone[1]	301.9	9.3	0.31	0.90	0.27	3.5	0.90
Shale	63.1	87.7	0.0081	0.93	0.54	3.0	0.96
Coarse Media in BSC Water							
Utelite	1474.9	3008.8	0.0038	1.00	0.73	27.1	0.99
Limestone	66.5	128.2	0.0040	0.98	0.69	1.4	0.98
Shale	104.0	170.0	0.0068	0.99	0.63	3.5	0.99
Ennis Gravel	84.4	138.2	0.0061	0.97	0.66	2.3	0.96
Lodgepole Biochar	467.6	456.0	0.040	0.81	0.34	65.3	0.69
Juniper Biochar	772.7	758.5	0.099	0.87	0.25	191.6	0.62

1. Langmuir and Freundlich isotherm equations fit only to portion of isotherm data prior to inflection point.
2. Freundlich affinity constant units depend on the value of , (see equation 3).

Utelite. Adsorption isotherms for coarse Utelite in DI water, fine Utelite in DI water, and coarse Utelite in BSC water are shown in Figure 19. In DI water, the fine particle size adsorbed significantly more P than the coarse particle size at all concentrations; the maximum adsorption capacity increased dramatically, from 367 mg kg^{-1} to 1189 mg kg^{-1}. Because smaller particles will have a larger surface area for a given mass, this is consistent with a surface area related adsorption process. An inflection point was also present in the adsorption isotherm of the fine size fraction in DI water, with adsorption capacity increasing sharply at concentrations greater than 30 mg L^{-1} P. This

may indicate that precipitation is an important mechanism for fine Utelite particles. The coarse Utelite also removed significantly more phosphorus from BSC water compared to DI water at concentrations above 10 mg L^{-1}. This may be due to the high concentrations of calcium in the BSC water, which would encourage precipitation of calcium phosphates, especially in combination with the high pH of the Utelite material. At high concentrations, the slope of isotherm for coarse Utelite in DI water appeared to flatten, indicating that a maximum adsorption capacity was reached. However, the adsorption capacity of fine Utelite in DI water and coarse Utelite in BSC water did not appear to reach a maximum value in the concentration range tested in these experiments, as shown by the steep isotherm slopes at high concentrations.

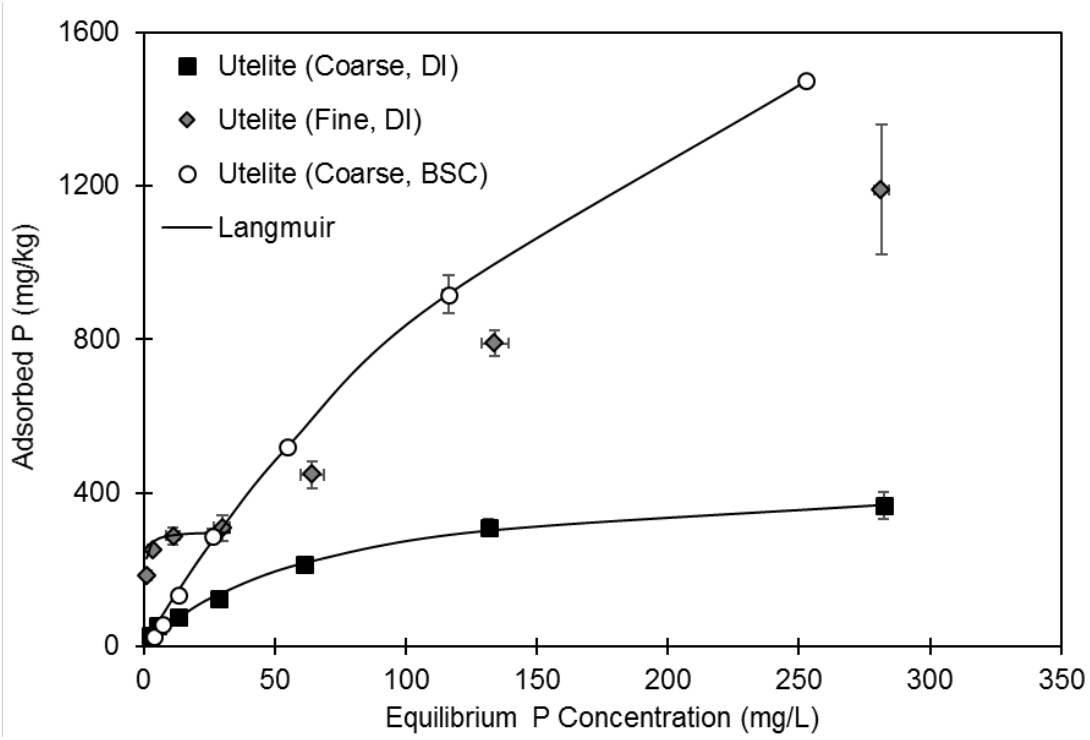


Figure 19. Adsorbed P versus equilibrium aqueous P concentration of coarse and fine Utelite in DI water, and coarse Utelite in BSC water. Error bars represent standard error (n=3).

Limestone. Adsorption isotherms for coarse limestone in DI water, fine limestone in DI water, and coarse limestone in BSC water are shown in Figure 20. Similar to Utelite, the fine limestone adsorbed more P than the coarse limestone in DI water, but this was only significant at concentrations above 80 mg L^{-1}. In DI water tests, both size fractions exhibited inflection points similar to Utelite near an equilibrium P concentration of 30 mg L^{-1}. This may indicate that precipitation is a dominant process for limestone in DI water at higher concentrations. However, the adsorption capacity of coarse limestone was significantly lower in BSC water compared to DI water at equilibrium concentrations greater than 80 mg L^{-1}. In addition, no inflection point is present in the coarse limestone in BSC water isotherm. At low concentrations, the adsorption capacity was slightly higher in BSC water compared to DI water for coarse media. Langmuir and Freundlich equations fit the adsorption isotherm in BSC throughout all equilibrium concentrations, but did not fit isotherms in DI water when the equilibrium concentration was greater than 30 mg L^{-1}. Based on the slope of the adsorption isotherms, limestone did not appear to reach a maximum adsorption capacity in the concentration range tested in these experiments, although the coarse limestone in BSC water appeared close with the isotherm slope flattening slightly at high concentrations.

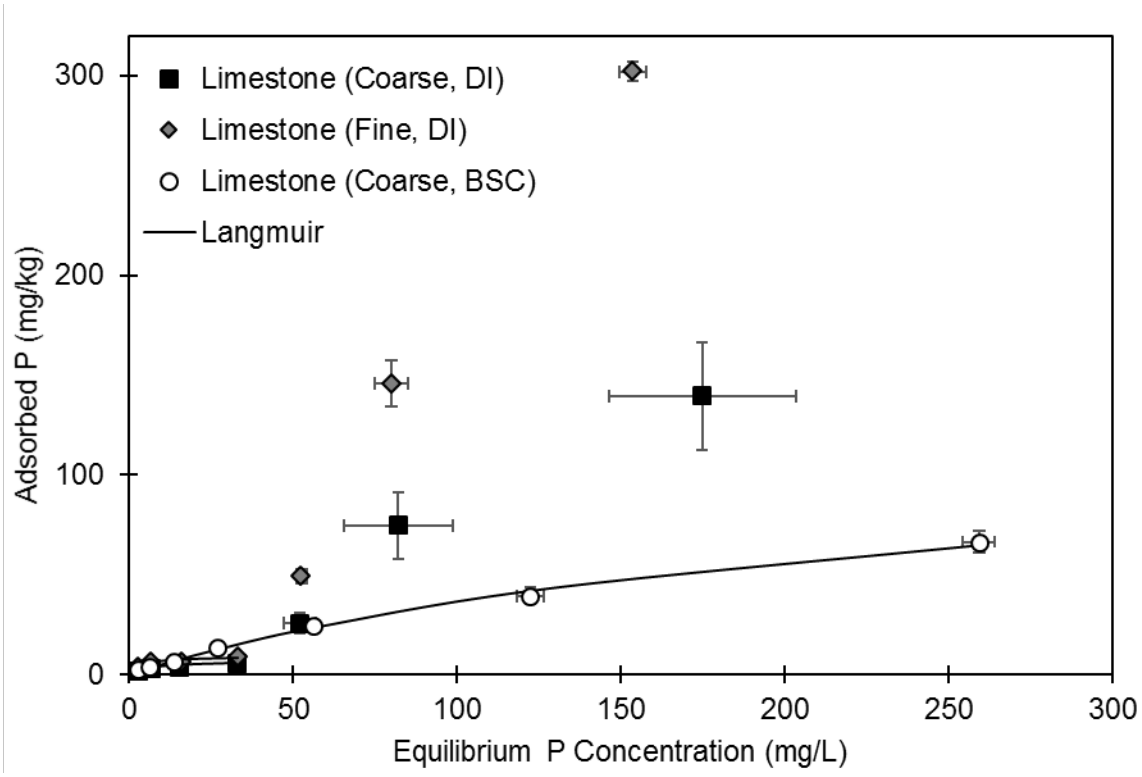


Figure 20. Adsorbed P versus equilibrium aqueous P concentration of coarse and fine limestone in DI water, and coarse limestone in BSC water. Error bars represent standard error (n=3).

Shale. Adsorption isotherms for shale are shown in Figure 21. The adsorption capacity of fine shale in DI water was slightly greater than coarse shale at concentrations between 0-150 mg L^{-1}, but this was only significant between 50-150 mg L^{-1}. Above 150 mg L^{-1}, the adsorption capacity of fine shale was slightly lower than coarse shale in DI water, but this was not significant. Overall, there was little difference between fine and coarse shale in DI water. However, the adsorption capacity of coarse shale in BSC water was greater than in DI water at all concentrations, and this was significant above 20 mg L^{-1}. Langmuir and Freundlich equations fit all isotherm curves well. Shale did not appear to reach a maximum adsorption capacity in the concentration range tested in these experiments.

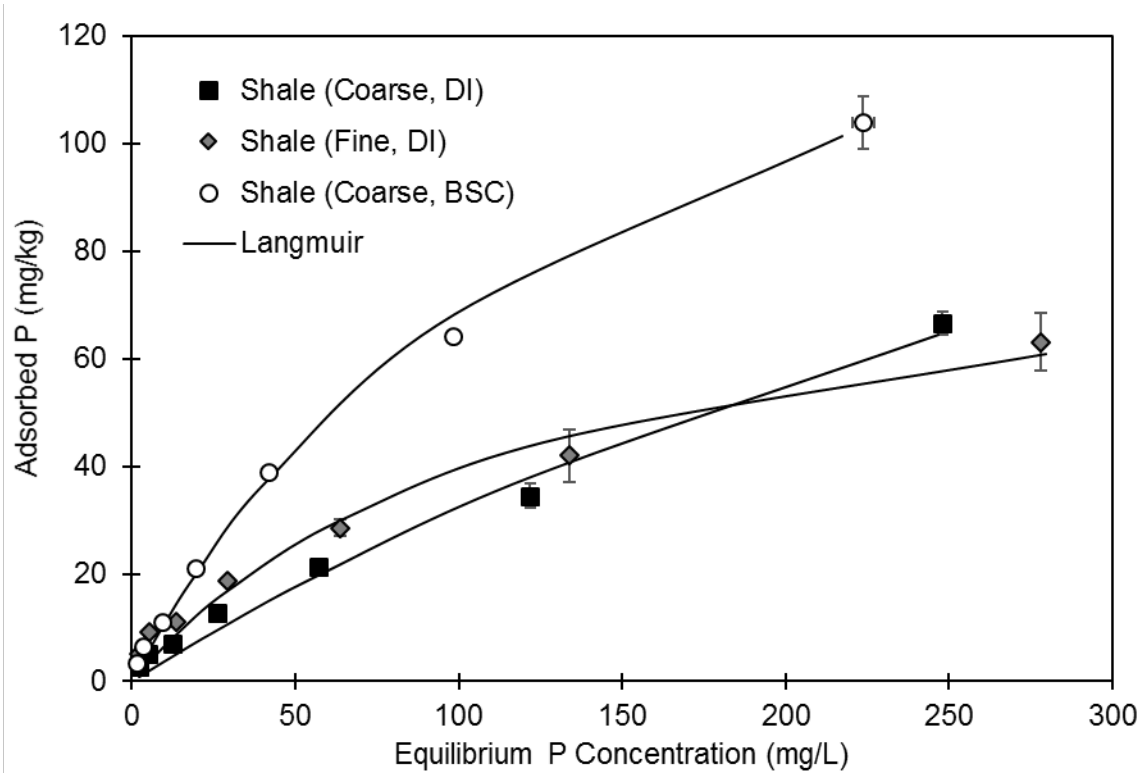


Figure 21. Adsorbed P versus equilibrium aqueous P concentration of coarse and fine shale in DI water, and coarse shale in BSC water. Error bars represent standard error (n=3).

Gravel. Adsorption isotherms for coarse gravel in DI water and BSC water are shown in Figure 22. The adsorption capacity was slightly greater in BSC water compared to DI water at low concentrations, and significantly greater at concentrations above 20 mg L^{-1}. The Langmuir equation fit the BSC water isotherm well, but did not represent the DI water isotherm well due to an inflection point present near an equilibrium P concentration of 100 mg L^{-1}. Gravel did not appear to reach a maximum adsorption capacity in the concentration range tested in these experiments.

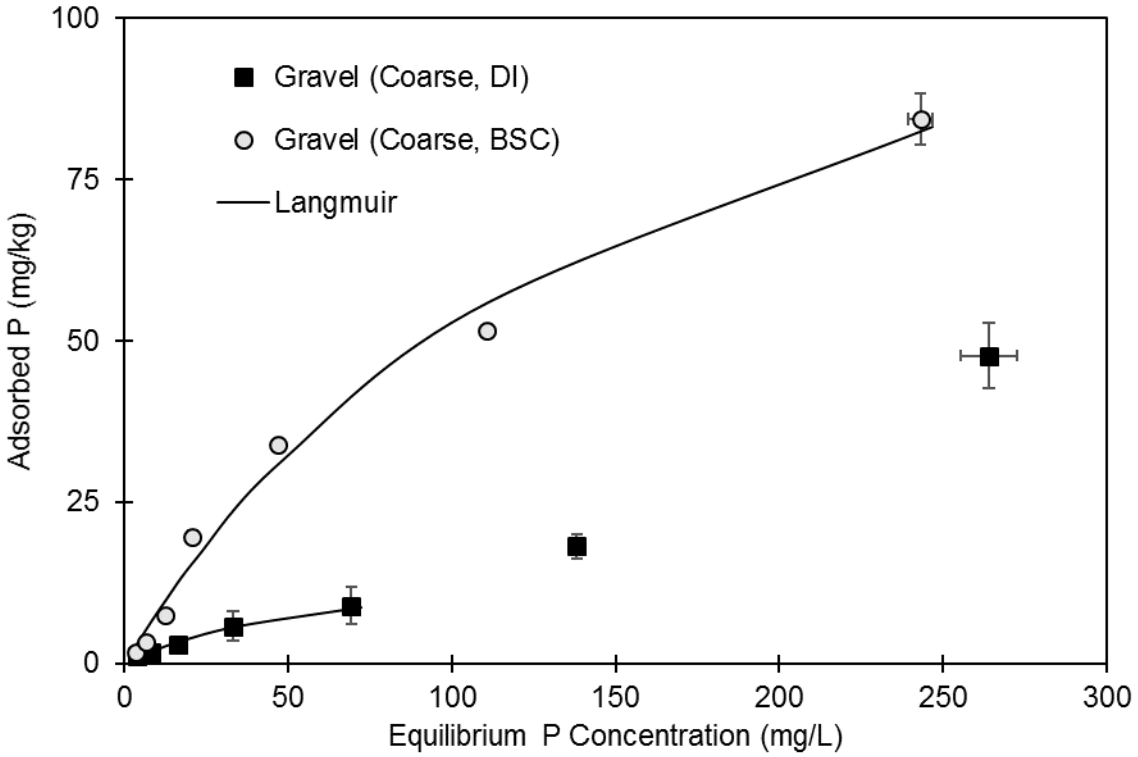


Figure 22. Adsorbed P versus equilibrium aqueous P concentration of coarse gravel in DI water and BSC water. Lines represent fitted Langmuir isotherm curves. Error bars represent standard error (n=3).

Dolomite. The adsorption isotherm for coarse dolomite in DI water is shown in Figure 23. Langmuir and Freundlich equations did not fit the isotherm well due to an inflection point near 150 mg L^{-1}. The adsorption behavior of the dolomite was similar to that of gravel, as indicated by the adsorption capacities and the Langmuir and Freundlich equation constants. Dolomite did not appear to reach a maximum adsorption capacity in the concentration range tested in these experiments.

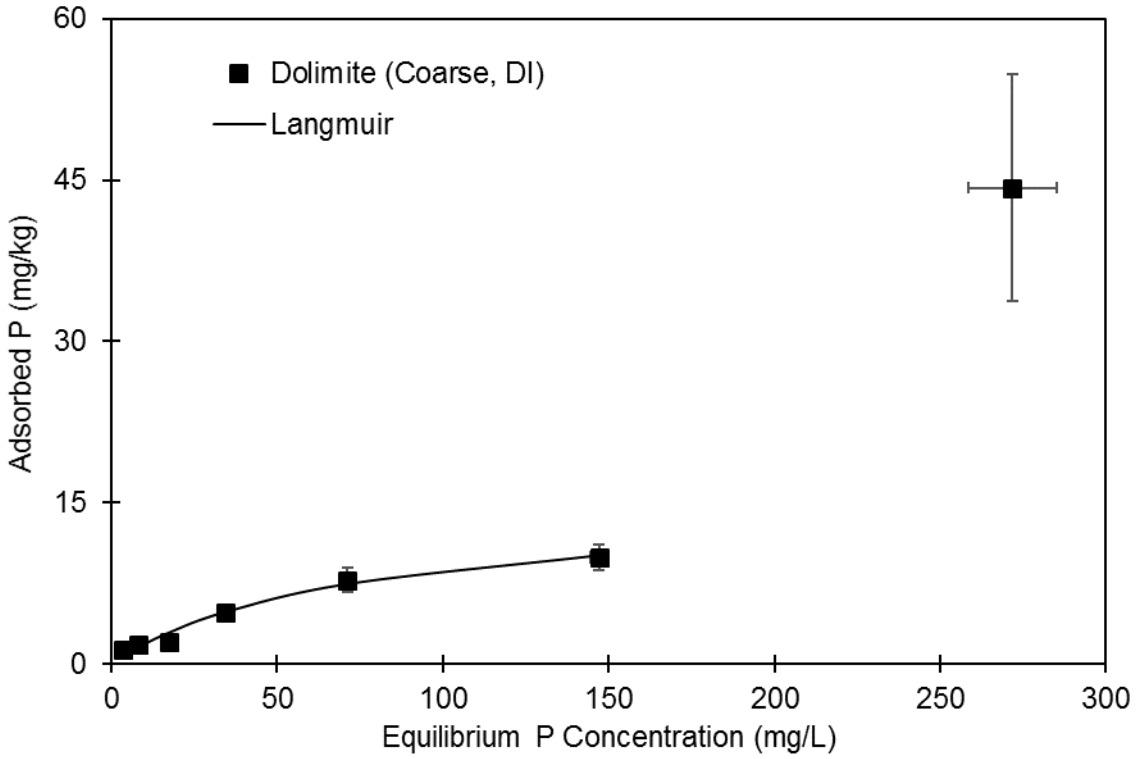


Figure 23. Adsorbed P versus equilibrium aqueous P concentration of coarse dolomite in DI water, with Langmuir isotherm curve. Error bars represent standard error (n=3).

Biochar. Adsorption isotherm for coarse juniper and lodgpole biochars in BSC water are shown in Figure 24 and Figure 25. These isotherms were characterized by steep initial slopes reaching maximum adsorption capacities at relatively low P concentrations. Both biochars showed a maximum adsorption at concentration between 50 – 150 mg L^{-1}, with adsorption decreasing slightly at higher concentrations. Because the Langmuir isotherm levels off at a maximum adsorption capacity (q_0), the Langmuir equation fit the data slightly better than the Freundlich equation but neither equation can capture a decreasing adsorption capacity with increasing equilibrium concentration.

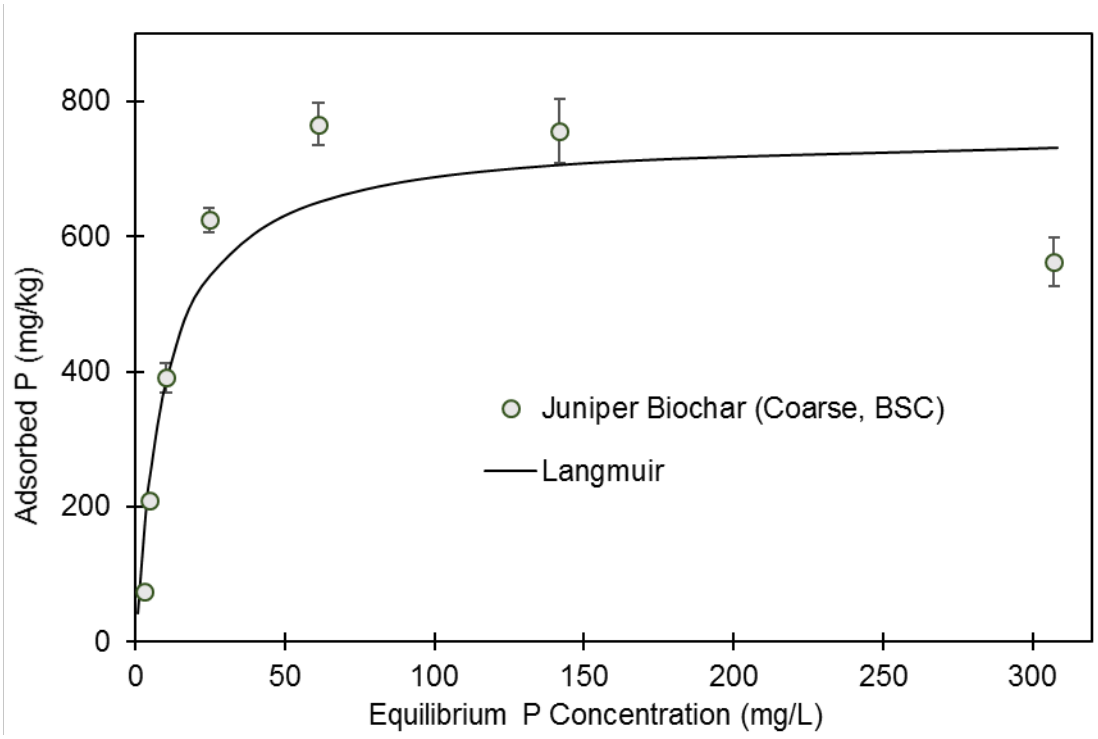


Figure 24. Adsorbed P versus equilibrium aqueous P concentration of coarse juniper biochar in BSC water with Langmuir isotherm curves. Error bars represent standard error (n=3).

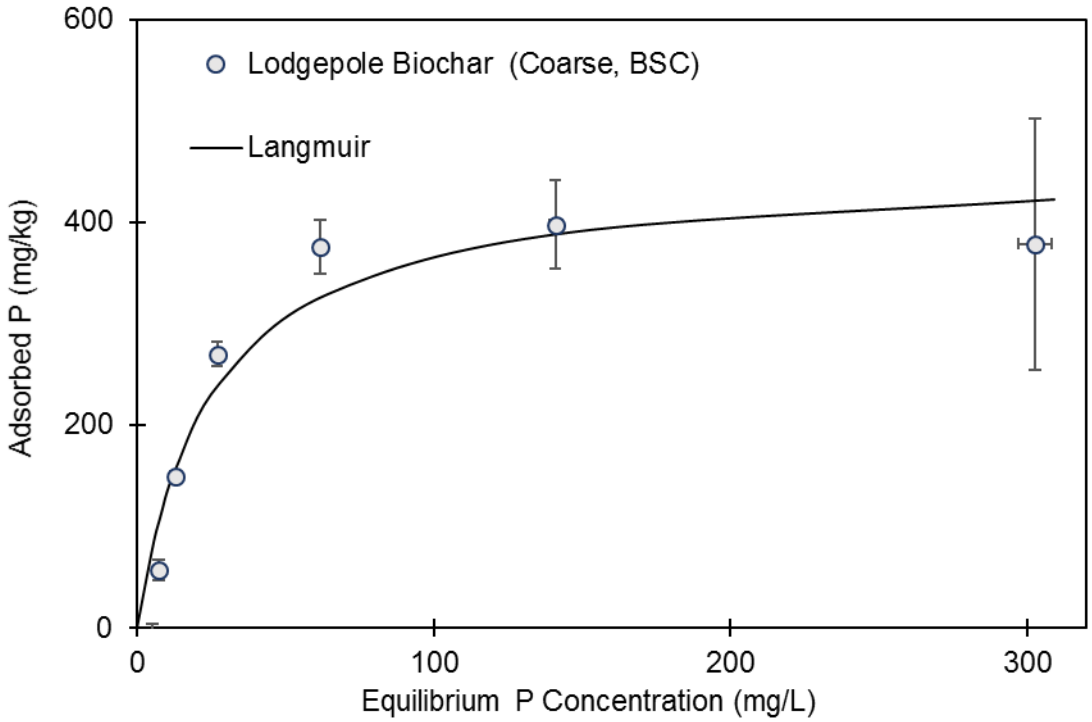


Figure 25. Adsorbed P versus equilibrium aqueous P concentration of coarse lodgepole biochar in BSC water with Langmuir isotherm curves. Error bars represent standard error (n=3).

Precipitation in Blaine Spring Creek Water

Experiments to assess the precipitation of P in Blaine Spring Creek water were conducted by adding known quantities of P directly to the water and measuring the concentration after 24 hours with no media present. As shown in Figure 26, very little precipitation occurred at initial P concentrations less than 20 mg L^{-1}. The decrease in P concentrations at initial concentrations less than 10 mg L^{-1} was not significant. At initial concentrations higher than 20 mg L^{-1}, 15–22% of the phosphorus in solution precipitated after 24 hours of equilibrium time, with a maximum of 46 mg L^{-1} precipitated at an initial concentration of 320 mg L^{-1}.

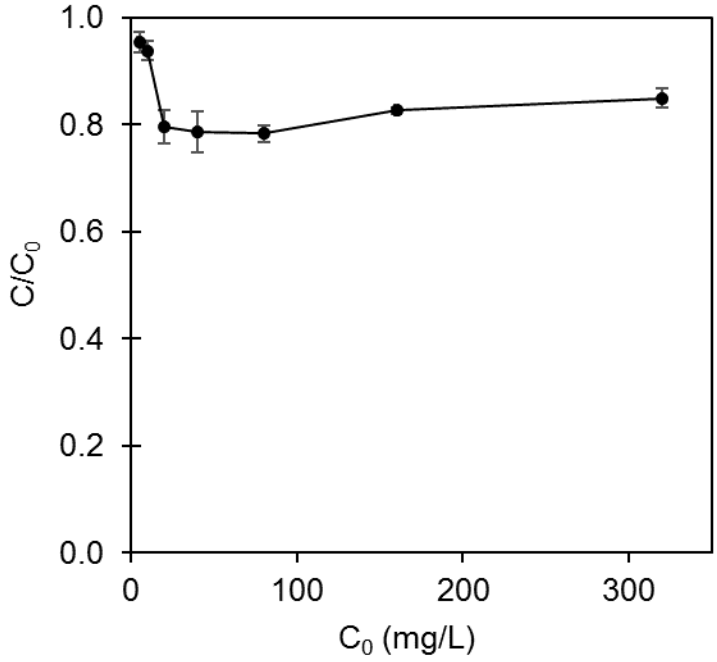


Figure 26. Ratio of equilibrium P to initial P versus initial P concentration in BSC water (without media).

To determine whether the difference in adsorption between the two types of water onto the same media could be attributed purely to precipitation in BSC water, the adsorption isotherms in DI water were increased by the quantity of P precipitated in BSC water at the same initial concentration. The adjusted isotherm would be expected to be similar to the BCS isotherm if spontaneous precipitation in BSC water was the sole difference between water types. However, the DI water isotherms were not similar after adjustment; the adjusted adsorption capacity of Utelite, shale, and gravel in DI water was still less than in BSC water, while the adsorption capacity of limestone was greater. This indicates that the BSC water does not simply precipitate more P from solution, but that the BSC water influences the adsorption behavior and/or the media influences the precipitation reactions.

Continuous Flow Tests

Continuous flow column experiments were conducted with Utelite and lodgepole biochar, due to their high adsorption capacities in batch tests. Lodgepole biochar was chosen over juniper biochar due to its lower pH. Gravel was also tested in the column configuration to provide a baseline performance comparison. Gravel and biochar columns were run for just under one month, and Utelite columns were run for just over two months. For the first phase, all columns were run with a target HRT of 24 hours. The flow rate was measured every 5–10 days and, due to differences in pump cartridges and degradation of pump tubing, varied with time during the experiment, thus causing changes in the actual HRT. Average HRTs were therefore calculated using time-averaged flow rates through each phase (Table 9). Average hydraulic residence times generally varied by 10-30% between column replicates, with the exception of the biochar which varied by 50% due to high degradation of one of the pump tubing lines which caused the flow rate to drop to near zero flow twice during the experiment.

Table 9. Column hydraulic residence time.

		Average HRT (hr)	
Column	Replicate	Phase 1	Phase 2
Gravel	1	21.3	-
	2	29.8	-
	3	30.1	-
	Average	**27.1**	-
Utelite Layered	1	25.7	14.2
	2	29.4	15.8
	3	21.0	16.4
	Average	**25.4**	**15.5**
Utelite Mixed	1	26.0	14.1
	2	28.3	15.0
	3	28.6	14.8
	Average	**27.6**	**14.6**
Lodgepole Biochar	1	25.6	-
	2	41.3	-
	3	29.2	-
	Average	**32.1**	-

Column influent and effluent phosphorus concentrations are shown in Figure 27. To account for differences in flow rates and pore volumes between columns and sampling times, sampling time was normalized to the calculated hydraulic residence time (θ_h) for that time period for all plots. This normalized time is equal to the number of pore volumes that have passed through each column. Influent P concentrations tended to decrease slightly after fresh solutions were made, likely due to precipitation within the feed container. Effluent concentrations were close to zero initially but breakthrough occurred quickly in the gravel and biochar columns, with concentrations rising to within 80% of the influent concentration after 4.4–4.9 and 4.9–6.9 pore volumes, respectively. After this quick initial increase, effluent concentrations in the gravel columns stabilized at 92 – 94% of the influent concentrations. Complete breakthrough was observed in the

biochar columns, with effluent P equal to influent concentrations. Several periods of decreasing effluent concentration were observed in the gravel and biochar columns, but could not be associated with any changes in column operation. There were no significant differences between the total phosphorus removal in the gravel and biochar columns.

Breakthrough in the Utelite columns began after 2-5 pore volumes, but concentrations rose slowly compared to the nearly complete breakthrough seen in the gravel and biochar columns. At the end of the experiment, the effluent concentration of the Utelite columns was between 72-79% of the influent concentration, and the rate at which the effluent concentration was increasing had slowed. There was no significant difference between the layered and mixed Utelite configurations. Effluent concentrations decreased several times in the Utelite columns, typically after increases in column HRT due to decreased pump flow and after periods of column resting. Column effluent P concentrations were less in the first sampling after the transition to phase 2, which can be attributed to the three-day resting period between phases. Subsequent samples showed a sharp increase in effluent P concentrations compared to phase 1.

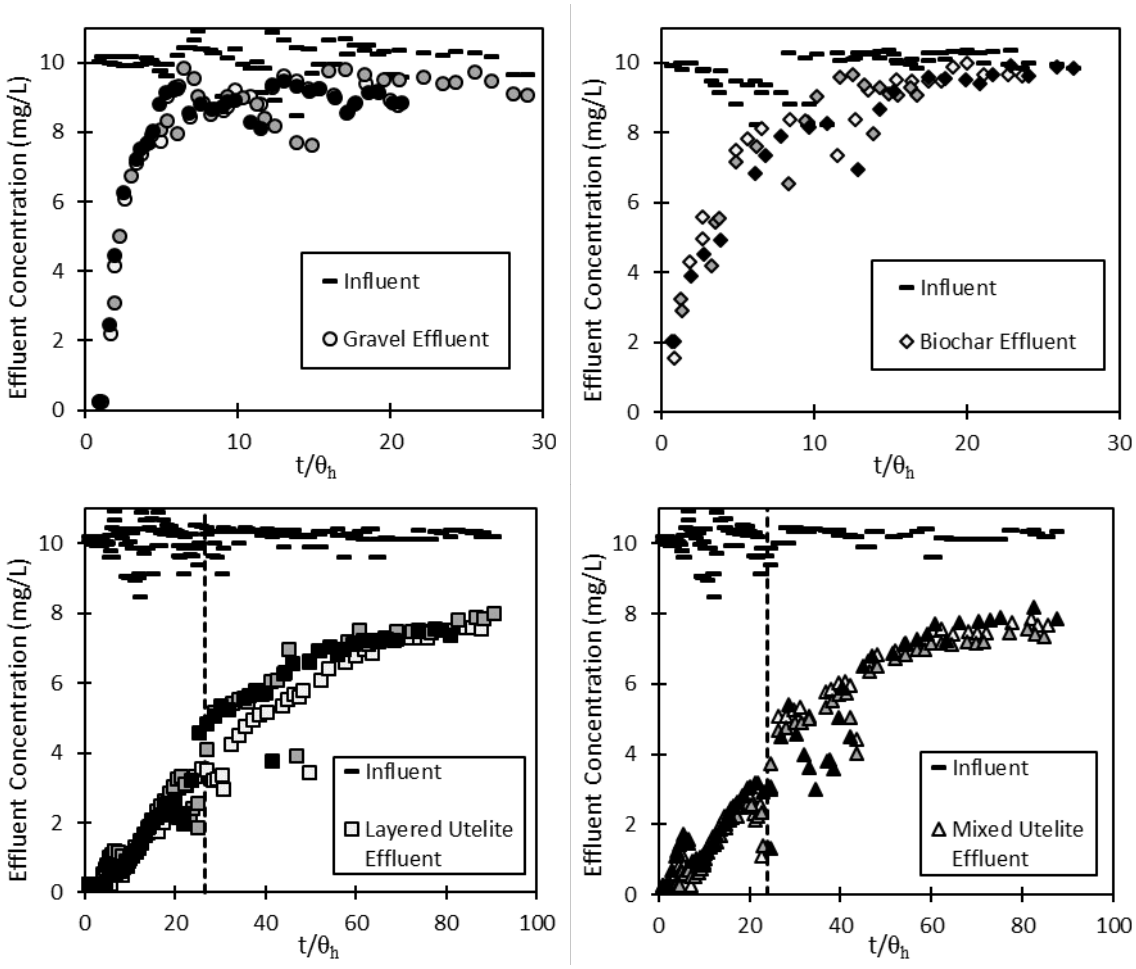


Figure 27. Column influent and effluent P concentrations. Vertical dashed line represents transition between phase 1 and phase 2 in the Utelite columns.

The pH of column influent and effluent was monitored throughout the experiment, shown in Figure 28. Influent pH varied between 7.7 and 8.2, and generally increased after fresh feed solution was made. Effluent pH from the gravel and biochar columns remained below 9 for the duration of the experiment. Two of the layered Utelite columns and one of the mixed Utelite columns had effluent pH above 9 for the first 2 – 5 pore volumes, after which effluent pH remained below 9. The transition to a shorter HRT in phase 2 did not appear to affect the effluent pH.

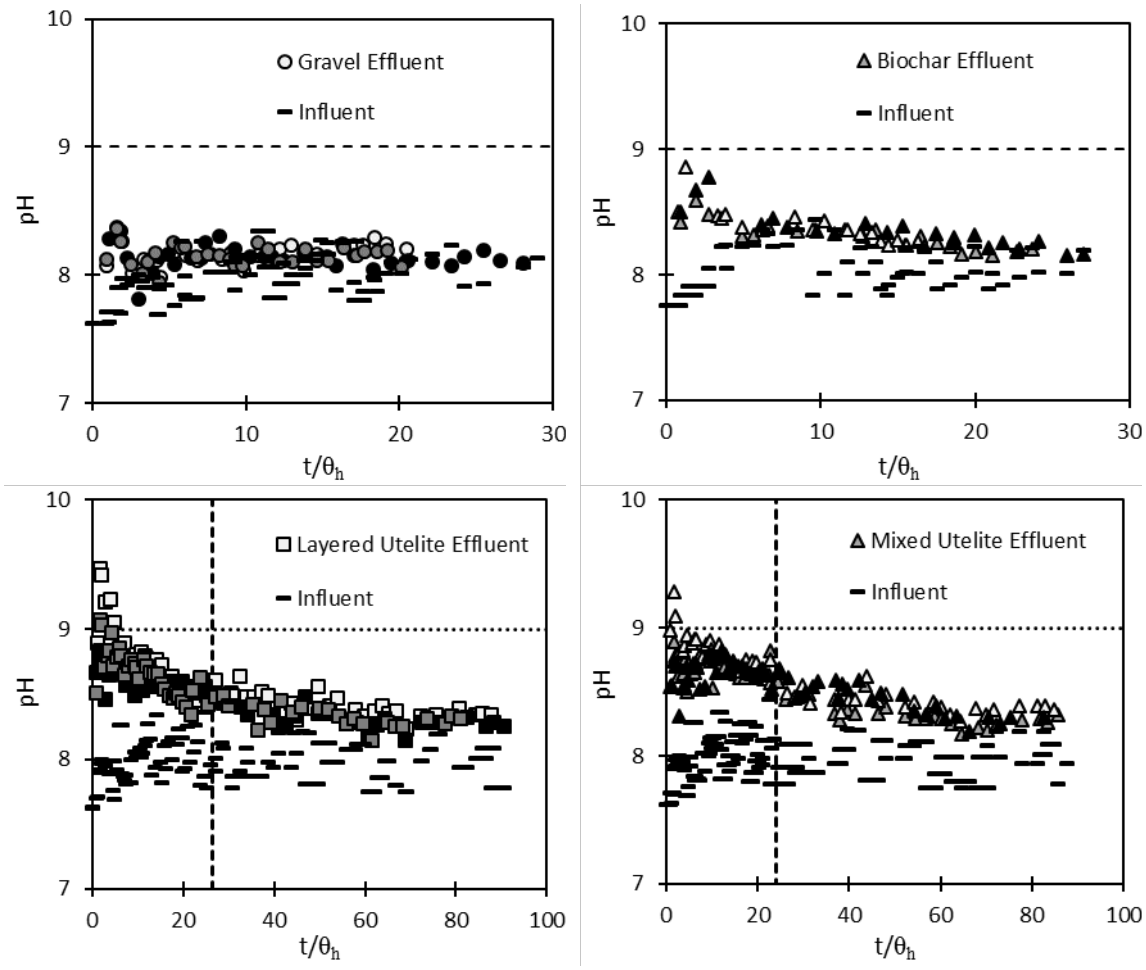


Figure 28. Column influent and effluent pH. Horizontal dashed line shows typical discharge pH limit of 9. Vertical dashed line represents transition between phase 1 and phase 2 in Utelite columns.

Effluent concentrations and flow rates were used to calculate cumulative P removal by each column, shown in Figure 29. To determine the volume of water and thus mass of P added and removed between sampling times, the flow rate was calculated at each sampling time by assuming that the flow rate varied linearly between flow measurements. Cumulative P added to and removed by each column was normalized to the nominal column volume, which was 0.75 L. To avoid confusion with concentration values, P addition and P removal by columns is reported in units of grams of P per cubic

meter net reactor volume (g P m^{-3}). The phosphorus removal efficiency of the gravel and biochar columns decreased quickly, reaching 50% cumulative removal after 22-30 g P m^{-3} was added to the columns. The gravel columns were terminated after reaching a steady state of 6-9% P removal, corresponding an effluent P concentration of 8.8-9.5 mg L^{-1}. The biochar columns were terminated after complete breakthrough and no additional P removal occurred. The Utelite columns maintained cumulative mass removal greater than 90% up to about 72 g P m^{-3} had been added, and were able to continuously remove P throughout the experiment. Removal efficiency decreased to 50% cumulative P input only after 350 – 388 g P m^{-3} was added at which point the Utelite column tests were terminated. At that time, phosphorus removal capacity had not been saturated, and the columns were continuing to remove approximately 20% of the influent P.

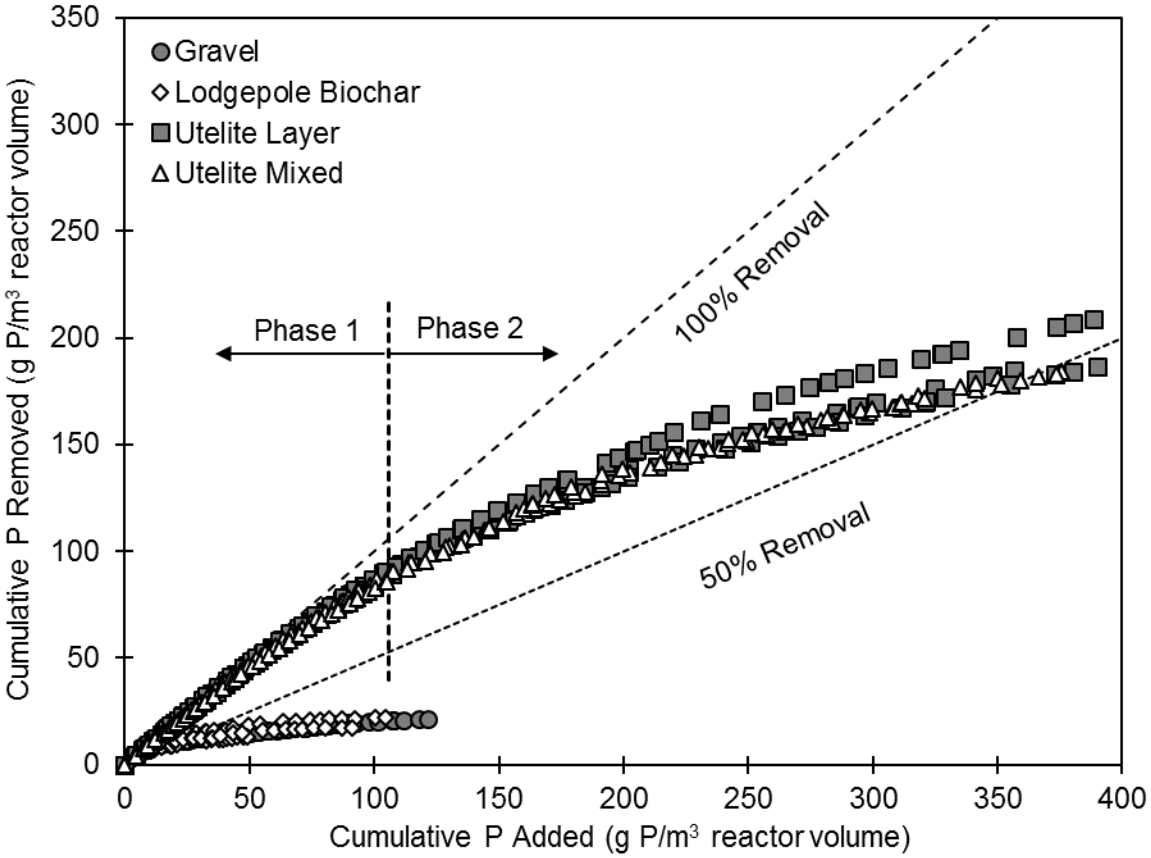


Figure 29. Cumulative P removed versus cumulative P added, normalized to the column reactor volume. Vertical dashed line represents average point of transition between phase 1 and phase 2 (range 93 – 135 mg P/L reactor volume).

Discussion

Effect of Media Characteristics

Although media composition is sometimes related to phosphorus removal, these experiments found no correlation between adsorption capacity and content of calcium, magnesium, iron, or aluminum in the media (Figure 30). Calcium is the most common element associated with phosphorus removal, but specific calcium-compounds, particularly CaO and $Ca(OH)_2$, are known to be more closely related to phosphorus adsorption than the presence of the calcium alone (Vohla et al., 2011). This may explain

the high removal capacity of Utelite, as the high temperature manufacturing process of lightweight aggregates can transform calcium compounds into the more reactive calcium oxides (Zhu et al., 1997). It is likely that specific compounds of magnesium, iron, and aluminum are also more critical than the mere presence of these elements. High pH is also associated with high CaO content (Vohla et al., 2011), which may explain a weak but noticeable correlation between pH and maximum removal capacity found in this experiment ($r^2 = 0.56$). The effect of pH is not decisive however, as low pH typically predicts low adsorption capacity, but high pH does not necessarily indicate high adsorption capacity (Cucarella & Renman, 2009).

Arias et al. (2001) found a correlation between the calcium content and P removal capacity for various types of sands. It is possible that the form of calcium will be the same in similar materials, so that the elemental calcium reflects the total calcium available for reaction. Both the calcium content and P removal capacity of the gravel and dolomite used in this study was less than in other studies using gravel and dolomite media which is consistent with an assumption of similar calcium form in similar media (Arias et al., 2001; Prochaska & Zouboulis, 2006; Tang et al., 2009; Xu et al., 2014).

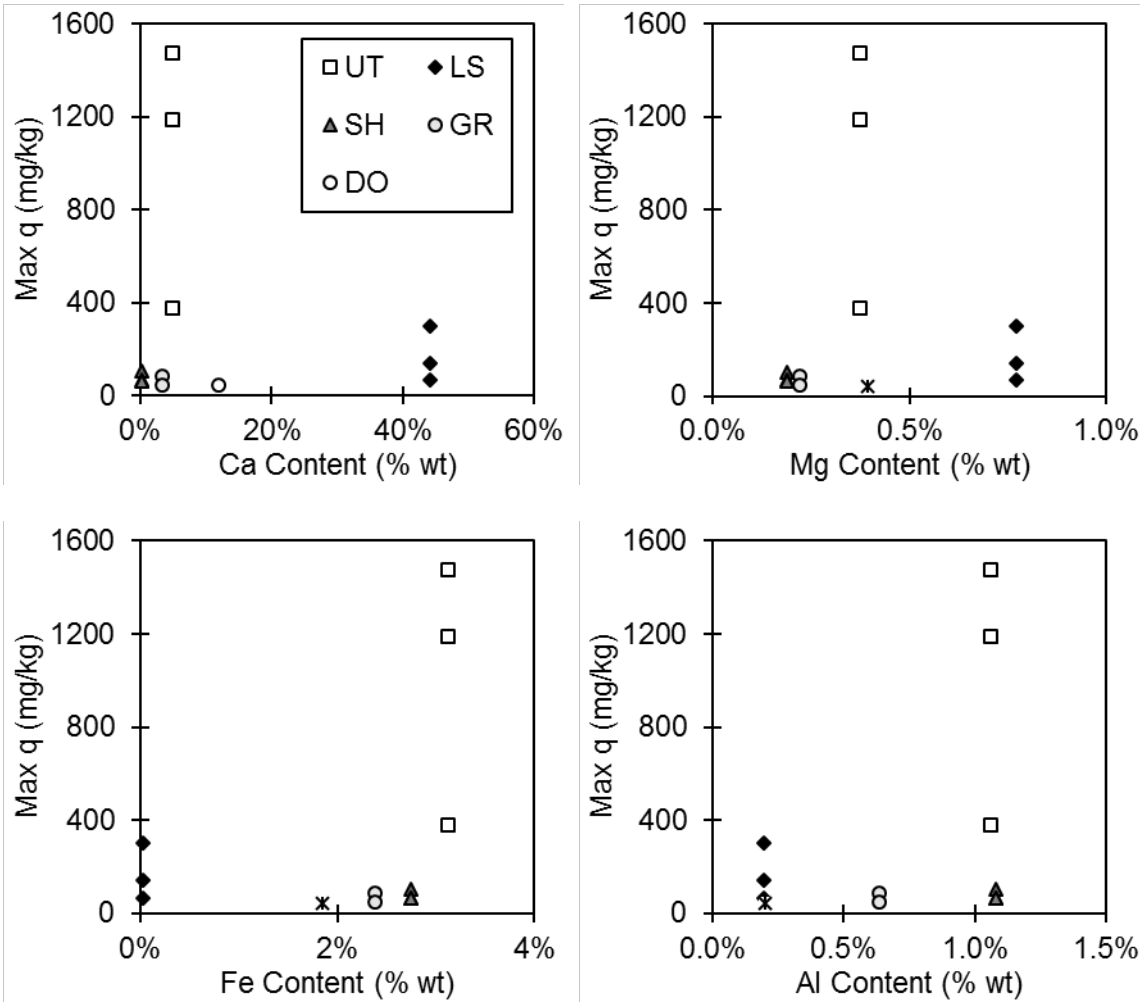


Figure 30. Relationship between calcium, iron, magnesium, and aluminum content on maximum adsorption capacity of Utelite (UT), limestone (LS), shale (SH), gravel (GR), and dolomite (DO). Maximum adsorption capacities for each set of batch experiments performed with each media are shown (fine media in DI water, coarse media in DI water, coarse media in BSC water).

Grain size had a large effect on the adsorption capacity of Utelite and limestone, but little effect on shale adsorption. The maximum adsorption capacity of fine Utelite was over three times greater than the coarse Utelite in DI water, which is consistent with another study comparing two size fractions of Utelite (Cyrus & Reddy, 2010). The effect of grain size observed in our study is also consistent with the results of Zhu et al. (1997),

who found that Utelite 0 – 2 mm in grain size had a maximum adsorption capacity of 3460 mg kg^{-1}, over twice the adsorption capacity found for the 0.841 – 2.00 mm grain size in our DI water experiments. Only one other study tested a limestone of a similar size fraction (0.25 – 2 mm); their maximum adsorption capacity was similar to the maximum adsorption capacity in BSC water, but the maximum concentration tested was 25 mg L^{-1} (Johansson, 1999) compared to 320 mg L^{-1} in our study. It is possible that the shale tested in our experiments had a high internal porosity, so that the internal surface area was available for adsorption and the exterior surface area (which increases with smaller grain sizes) is less important. However, the internal porosity was not measured and so this cannot be confirmed.

While most studies confirm the effect of grain size for a specific media, the source of a specific material (e.g. limestone or shale) can be equally important, likely due to different mineralogies. The adsorption capacity of the limestone in all three batch tests (coarse media in DI water, coarse media in BSC water, and fine media in DI water) in our study was at the lower range of literature reports, performing poorly compared to the limestone tested in other studies (Drizo et al., 1999; Johansson, 1999; Zhou & Li, 2001). Small grain sizes in our study also performed worse than large grain sizes in other studies. Similarly, the shale tested in our experiments had much lower adsorption capacity than shale tested by others (Drizo et al., 1999; Zhou & Li, 2001), and unlike another study (Tang et al., 2009), grain size had little effect on the adsorption capacity of our shale.

Manufactured products such as Utelite would be expected to exhibit less variation compared to natural materials from different sources, and our results for Utelite are similar to other published reports (Cyrus & Reddy, 2010; Zhu et al., 1997). The adsorption capacity of biochar varies greatly depending upon feedstock and production characteristics, with some biochars showing no phosphorus adsorption capacity and some engineered biochars removing up to 100,000 mg kg^{-1} (Chintala et al., 2014; Sarkhot et al., 2013; Yao et al., 2013; Yao et al., 2012). However, the biochars tested in our experiments had adsorption capacities similar to woody biochars tested by others (Chintala et al., 2014; Sarkhot et al., 2013). As discussed above, the limestone and shale had adsorption capacities at the low end of literature reports. The dolomite and gravel were also at the low end of literature reports (Arias et al., 2001; Prochaska & Zouboulis, 2006; Tang et al., 2009; Xu et al., 2014). These results show that predicting phosphorus removal capacity based on a generic classification of media type is difficult at best. While small grain sizes generally increase adsorption capacity and should be used, this effect may be small for some media. This research highlights the benefit of testing locally available media for new applications.

Effect of Water Quality

The water used in batch experiments had a significant impact on the phosphorus removed by each media. For all media except limestone, adsorption capacity increased significantly in BSC water compared to DI water for the coarse size fraction. The adsorption capacity of limestone in BSC water was slightly higher than in DI water at concentrations below 80 mg L^{-1}, but significantly lower in BSC water at higher

concentrations. The BSC water has ionic strength of approximately 7.1 mmol L^{-1} (National Water Quality Monitoring Council, 2003) and high ionic strength is known to increase P adsorption by certain soils (Pardo et al., 1991), which may have contributed to the higher adsorption capacities observed in BSC water. The BSC water also had high concentrations of calcium ions (52 mg L^{-1}) and magnesium ions (21 mg L^{-1}), which may have increased the precipitation of calcium and magnesium phosphates. White precipitates were observed in the higher concentration batch tests in BSC water, both with and without media. The decrease in P after 24 hours at initial concentrations greater than 20 mg L^{-1} in BSC water without media (Figure 26) suggests that phosphate precipitation did occur.

The poor performance of limestone in BSC water compared to DI water may be due to the complex role pH plays in precipitation. In batch tests using DI, the limestone isotherms exhibited inflection points similar to those observed in other studies using limestone and calcite (Cole et al., 1953; Freeman & Rowell, 1981; Zhou & Li, 2001). This inflection point has been associated with a transition between physico-chemical adsorption and precipitation processes, suggesting that precipitation dominates at P concentrations of 30 mg L^{-1} or greater (Freeman & Rowell, 1981). Regardless of media type, the equilibrium pH of batch tests in DI water was generally high at lower initial P concentrations and decreased as more P was added due to the higher buffering capacity of solutions with more P (Figure 31). In the BSC water the relation between initial P concentration and equilibrium pH was similar for all media, but with most media the pH was lower at the same initial P concentration compared to DI water (Figure 32). In the

case of limestone, the pH was approximately one unit lower in BSC water than in DI water, while the difference in water source was 0.5 units or less for the other media at high initial P concentrations. If precipitation was an important process for the limestone, it is possible that less precipitation occurred in the BSC water batch tests, as the solubility of calcium phosphates increases at low pH (see Figure 15). The role of pH on phosphorus removal is complex; water with low pH has also been observed to increase the dissolution of calcium from the calcite and dolomite, thus increasing phosphorus removal via precipitation (Xu et al., 2014). However, the BSC water was naturally high in calcium and magnesium thus a lower pH did not increase Ca and Mg availability, but did increase calcium phosphate solubility, thus potentially decreasing P precipitation.

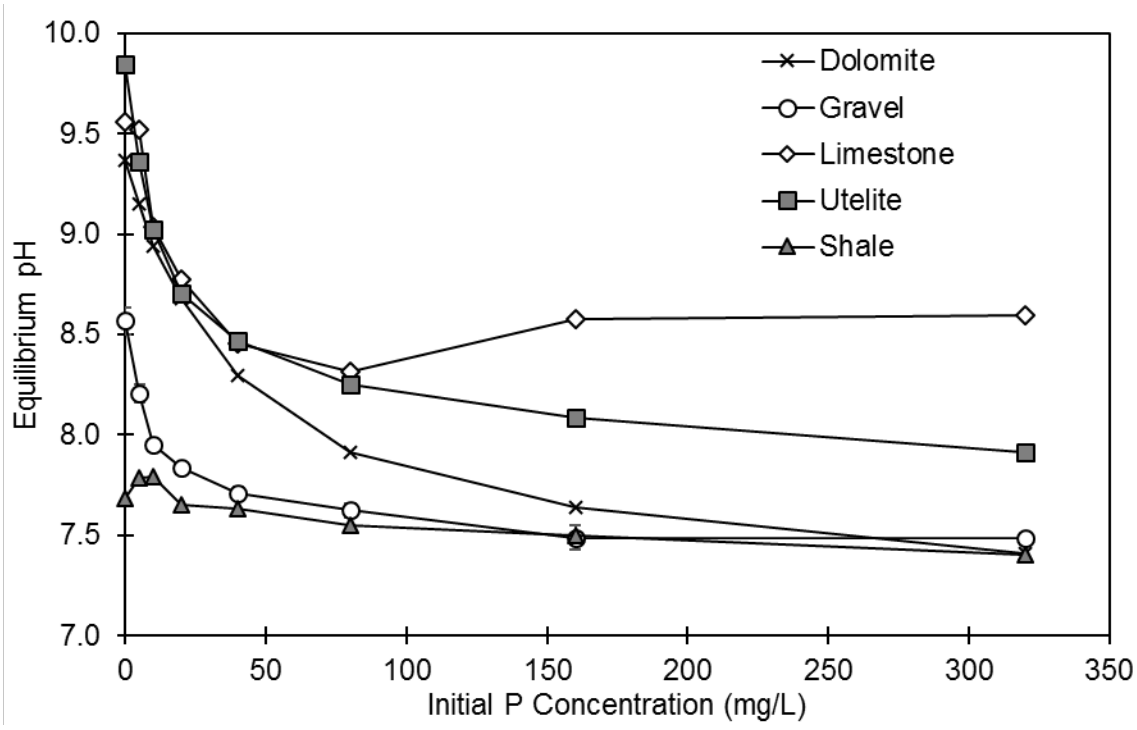


Figure 31. Equilibrium pH of batch adsorption tests in DI water.

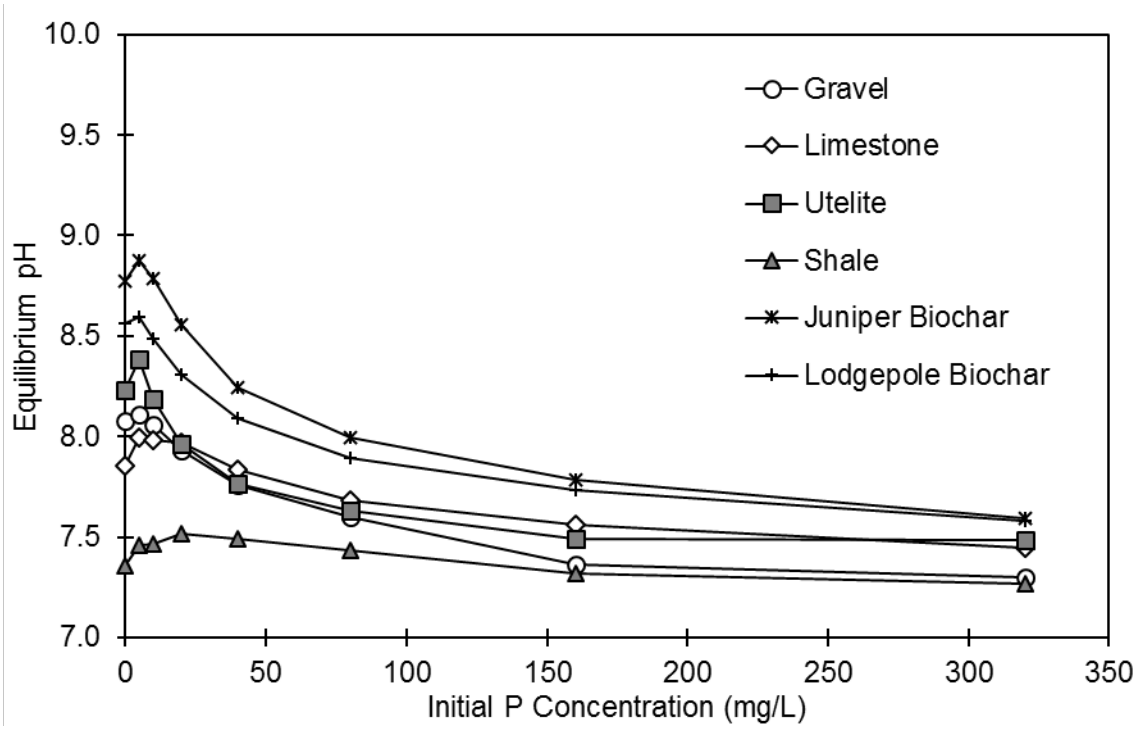


Figure 32. Equilibrium pH of batch adsorption tests in BSC water.

The influence of water chemistry on P removal makes direct comparison of results between studies difficult when different water sources are used. Although experiments conducted with DI water are easily replicated and can be directly compared, the results using BSC water showed significant differences compared to DI water and likely represent better estimates of adsorption capacities in the Ennis full-scale system. This reinforces the benefit of testing media for new applications.

Performance of Continuous Flow Columns

All columns removed nearly all the influent phosphorus during a short period immediately after startup. After this initial stage which was longer for Utelite, the P removal between media types varied dramatically, with the biochar columns rapidly decreasing to zero removal, the gravel columns rapidly decreasing to 6-9% removal, and

the Utelite columns very gradually decreasing to about 20% removal. The Utelite columns removed significantly more P than the gravel and biochar columns, but there was no significant difference between the two configurations of Utelite (mixed and layered) or between the biochar and gravel columns. The Utelite column removal was similar to reports by Cyrus and Reddy (2010), who found that columns receiving high P influent concentrations reached a steady state removal of 20 – 50% depending upon flow rate. Reduction in removal efficiency was also similar to other high performing media reported in the literature such as slag, apatite, limestone and shale which show high initial removal followed by gradually decreasing efficiency (Bellier et al., 2006; Chazarenc et al., 2010; Drizo et al., 2002). Unlike a similar experiment with slag, layering the Utelite did not appear to improve performance compared to a mixed system (Chazarenc et al., 2010). This may be because in our experiment Utelite was mixed with gravel rather than apatite and limestone, and our gravel likely has fewer calcium minerals to act as adsorption and precipitation seed sites downstream of the Utelite layer.

Batch versus Column Results. Although batch tests are often used to compare adsorption properties of different filter media, characteristics critical to full-scale operation are not necessarily captured in these experiments. Because gravel contributed towards some phosphorus removal in the Utelite and biochar columns, the total P removed by these columns could not be attributed to the Utelite and biochar alone. The quantity of P removed by the gravel in these columns was estimated by fitting a logarithmic curve to a plot of P removed by the gravel columns versus the number of pore volumes passed through the columns. The P removed by the gravel in Utelite and

biochar columns was then calculated using this fitted equation and subtracted from the total P removed to determine the P removed by the Utelite and biochar alone. Table 10 shows the quantity of P removed by each material in the columns and in batch experiments at 10 mg L^{-1}, which was estimated from the adsorption isotherm plots assuming a linear slope between data points bounding 10 mg L^{-1}.

The adsorption capacity of media in our continuous flow column experiments is poorly predicted by our batch experiment results despite similar residence times for reaction. If phosphorus removal in the columns were due to equilibrium adsorption processes as modeled by the Langmuir and Freundlich isotherms, the total phosphorus adsorbed by each material would be expected to be equal the adsorption in batch tests at the same influent concentration of 10 mg L^{-1}. Jenssen and Krogstad (2003) found that phosphorus removal by lightweight aggregates in full-scale systems can be predicted by batch tests at similar concentrations. However, our results suggest that batch experiments provide a lower bound for the total adsorption capacity under continuous flow. Batch tests approximated continuous flow adsorption only in lodgepole biochar columns, while the gravel and Utelite columns adsorbed nearly 2.5 more in the column compared to batch tests at 10 mg L^{-1}.

Table 10. Phosphorus removal in column experiments attributed to each material compared to phosphorus removal in batch tests at a similar P concentration.

Column	Replicate	P Added[a] (mg)	P Removed[a] (mg)	Gravel Mass (g)	Biochar or Utelite Mass (g)	P Removed by Gravel[b] (mg/kg)	P Removed by Biochar or Utelite (mg/kg)	Batch Test Removal @ 10 mg/L P (mg/kg)
Gravel	1	90.8	16.2	1119	-	14.4	-	
	2	68.4	14.7	1120	-	13.1	-	
	3	68.6	14.7	1120	-	13.2	-	
	Average	**75.9**	**15.2**	**1120**	**-**	**13.6**	-	**5.6**
Utelite Layer	1	285.40	138.51	950	100	17.5	1235.1	
	2	261.23	137.12	950	100	17.1	1227.0	
	3	286.31	155.68	950	100	17.4	1408.6	
	Average	**277.6**	**143.8**	**950**	**100**	**17.3**	**1290.2**	**477**
Utelite Mixed	1	281.28	137.88	970	100	17.3	1210.6	
	2	258.16	135.15	970	100	17.2	1206.4	
	3	276.69	137.44	966	100	17.3	1225.6	
	Average	**272.0**	**136.8**	**969**	**100**	**17.3**	**1214.2**	**477**
Lodgpole Biochar	1	79.61	16.55	300	100	13.4	125.2	
	2	48.94	13.05	291	100	11.8	96.1	
	3	68.20	13.03	335	100	13.0	86.7	
	Average	**65.6**	**14.2**	**309**	**100**	**12.8**	**102.7**	**98.7**

a. Phosphorus added and removed is cumulative amount at the end of the experiment.
b. Phosphorus removed by gravel in Utelite and lodgepole biochar columns was calculated using a best fit logarithmic curve representing removal in the gravel columns per pore volume passed.

Differences between batch and column tests may be explained by examining the phosphorus removal over time. Phosphorus adsorption is known to include both a rapid and slow reaction component (Jenssen & Krogstad, 2003). For phosphorus adsorption onto calcite, several authors have shown that the rapid phase is due to surface adsorption and the slow phase is due to precipitation, with the creation of calcium phosphate precipitates acting as additional adsorption sites and/or precipitation seeds (Cole et al., 1953; Freeman & Rowell, 1981). It is likely that the initial stage of complete removal was due to adsorption, and the longer duration of this initial stage observed in the Utelite columns reflects its higher adsorption capacity. The long-term, nearly steady-state phosphorus removal observed in Utelite and to a much smaller degree in gravel likely reflects ongoing precipitation. If hydroxyapatite is formed ($Ca_5(PO_4)_3(OH)$), the calcium present in the BSC water (52 mg L^{-1}) is sufficient to precipitate up to 24 mg L^{-1} P; if dicalcium phosphate ($CaHPO_4 \cdot 2H_2O$) is formed, 40 mg L^{-1} P may be precipitated. In the batch tests in BSC water without media, only 0.6 mg L^{-1} was precipitated at an initial P concentration of 10 mg L^{-1}, but at higher concentrations up to 46 mg L^{-1} of P was precipitated, indicating a high potential for precipitation. The high pH of Utelite likely resulted in more precipitation and higher long-term removal efficiency compared to the gravel column. Although the biochar column also had a high pH, as an organic material it is likely that fewer calcium minerals were available to act as precipitation seeds, which may be why no steady-state removal was observed. In addition, Sarkhot et al. (2013) suggested that phosphorus adsorption by biochar is due to exchange with surface hydroxyl groups. If biochar adsorption is an exchange process with little precipitation, the

performance in a column configuration would be expected to be similar to the batch test, as observed. This suggests that for media characterized by adsorption processes such as biochar, batch tests can accurately predict adsorption under continuous flow conditions, but for media which precipitates phosphorus, batch tests will underestimate adsorption under continuous flow.

Column Removal Kinetics

During the transition between the 24 hour and 12 hour residence time phases (phase 1 and phase 2 respectively) of the experiment, the Utelite columns were rested for 76 hours while full of liquid. This allowed an analysis of the removal efficiency before the resting period, at the end of the resting period, and after the resting period. Samples taken at the end of phase 1 just prior to the resting period had HRTs of 19.7 – 42.4 hours; samples taken at the end of the resting period had HRTs of 76 hours; and samples taken at the beginning of phase 2 just after the resting period had HRTs of 12.5 – 14.5 hours. The phosphorus removal efficiency (ratio of effluent P to influent P) was plotted against the HRT for each sample and fitted to the modified first order reaction equation (equation 4), shown in Figure 33. Parameter values for the modified first order equation are shown in Table 11. It is important to note that reaction kinetics may change over time as P is adsorbed, thus the equation parameters only reflect the reaction kinetics during the time when these samples were taken, 26 – 31 days into the experiment (corresponding to 22 – 34 pore volumes having passed through each column).

Based on the lower value of C^*, the mixed column appears to have a higher removal efficiency than the layered column at long residence times. However, the

difference in removal efficiency at 76 hours was not significant, and at the HRTs between 12 and 24 hours, no differences were observed between the column configurations. In addition, while preliminary batch tests showed little difference between 24 and 48-hour equilibrium times, the mixed column results suggests that residence times longer than 48 hours may be able to improve removal efficiency. Although this trend is not substantial, it is consistent with the precipitation of calcium phosphates on calcite, which has been shown to proceed gradually over days and weeks (Freeman & Rowell, 1981).

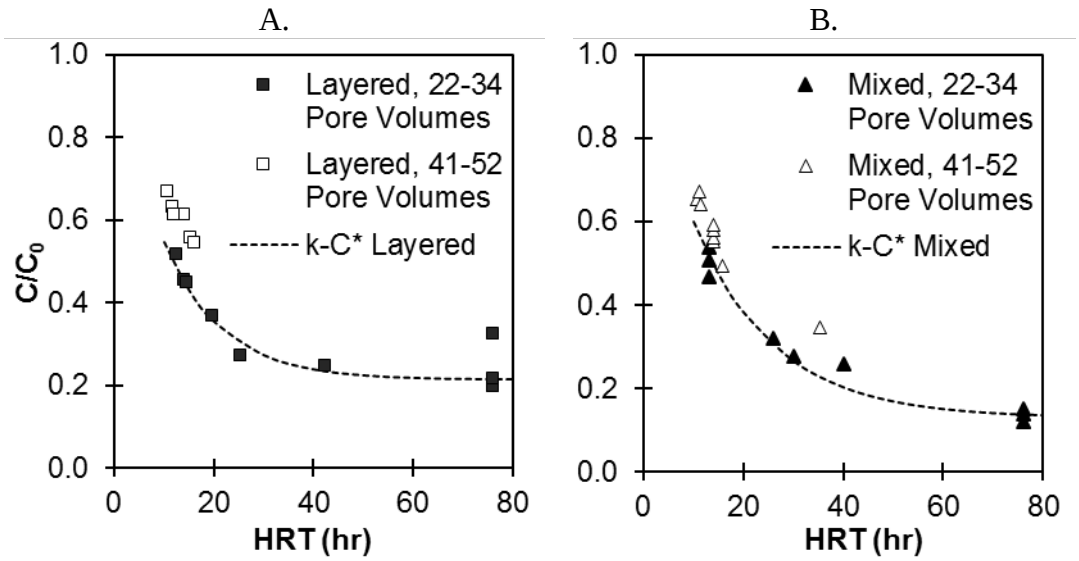


Figure 33. Phosphorus removal efficiency of layered Utelite columns (A) and mixed Utelite columns (B) versus HRT with k-C* model fit to the data of 22-34 pore volumes.

Table 11. Utelite column modified first order reaction kinetics.

Parameter	Layered Utelite	Mixed Utelite
K (hr^{-1})	0.086	0.062
C* (mg L^{-1})	2.14	1.31
r^2	0.91	0.98

Because the Utelite columns began operation removing nearly all the influent phosphorus, *C** was initially zero. As P is adsorbed *C** increases, reducing the total

removal efficiency. The modified first order reaction constants therefore only represent the reaction kinetics for the time period at which the data was collected, which was after 26 – 31 days into the experiment (after 22 – 34 pore volumes). Removal efficiency after 40 – 50 days into the experiment (corresponding to 41 – 52 pore volumes) is also plotted on Figure 33, and shows a slight decrease in removal efficiency compared to the data at 22 – 34 pore volumes, indicating a lower effective reaction rate. The slower reaction rate may be due to either an increase in C^* or a decrease in k. Because the modified first order equation includes two terms influencing the overall reaction rate, curve fitting is known to be difficult with variations in parameter values influenced by the statistical technique used and the spacing of data (Stein et al., 2007). Therefore, although it is clear that C* increases over time it is also possible that the removal efficiency decreases due to a change in the reaction rate term k.

CONCLUSIONS AND RECOMMENDATIONS

The three-stage treatment wetland constructed at the Ennis National Fish Hatchery has shown success in treating aquaculture wastewater, providing a long-term opportunity for studying treatment wetlands in southwest Montana. Preliminary operations exhibit excellent COD and phosphorus removal, complete nitrification and partial nitrogen removal. This system is the first of its kind in the United States to treat aquaculture wastewater, and these preliminary results suggest that this is a promising treatment solution for similar facilities.

The first two stages of the ENFH treatment wetland removed over 95% of influent phosphorus over the first two months of operations, but effluent concentrations will likely rise as the P adsorption capacity of the wetland media becomes saturated and the stage 1 sludge layer mineralizes producing more orthophosphate. To provide for long-term P removal, the treatment wetland was designed with a phosphorus removal stage, downstream of stage 1 and 2. This stage consists of three horizontal flow cells to be filled with phosphorus adsorbing media. To select the optimal filter media, seven different materials were tested for P adsorption capacity and characterized by elemental composition and pH tests. The three manufactured materials performed far better than the five natural materials tested. Phosphorous adsorption capacity did not correlate with the elemental composition of the material and only weakly correlated to pH. In addition, adsorption capacities for all natural materials was low compared to published reports of similar materials from different sources. Adsorption tests were therefore justified, and are recommended for finding locally available materials to use in new applications. Water

chemistry and particle size were also found to significantly influence P adsorption capacities. To provide the most accurate estimate of adsorption capacity under field conditions, adsorption tests should be conducted with similar media particle size, water chemistry, and retention times as to be used in the full-scale system.

Continuous flow column experiments were conducted to compare two of the top performing media (Utelite and lodgepole biochar) and gravel; the results revealed stark differences between the materials and between continuous flow and batch experiments. Adsorption capacity of Utelite and gravel found in column experiments was greater than in batch experiments, while biochar was approximately equal. This suggests that adsorption capacities determined under batch conditions may underestimate the P removal capacity of some materials compared to continuous flow conditions. Differences in behavior under continuous flow conditions is likely due to removal mechanisms. Batch adsorption capacity does appear useful to estimate a lower bound for the P removal capacity, if conducted at similar concentrations as the continuous flow tests. Adsorption capacity determined under batch conditions at high P concentrations or using the Langmuir maximum adsorption capacity overestimate the adsorption capacity under continuous flow, and should not be used. Continuous flow experiments provide useful information not necessarily captured in batch conditions, and are recommended for comparing potential filter media.

Based on its high phosphorus removal capacity in both batch and continuous flow experiments, Utelite is recommended as a filter media for the stage 3 of the ENFH treatment wetland. The Utelite media removed 477 mg P kg^{-1} in batch experiments and

1200 mg P kg^{-1} in continuous flow column experiments. Results of preliminary batch tests showed no difference between equilibrium times of 24 hours and 48 hours, indicating that equilibrium had been reached in the 24-hour batch tests. Continuous flow experiments more closely represent full-scale conditions, and adsorption capacities found under these experiments should be used for longevity estimates. If current wastewater flow rates are maintained the HRT in the third stage cells will be approximately 46 hours, which should result in higher P removal efficiency compared to the results of the column experiments which were conducted primarily at HRTs of 12 and 24 hours. However, a variety of other factors influence the P removal under full-scale conditions, and so the adsorption capacity found in continuous flow experiments provides the best estimate.

Each filter cell will hold 5.1 m^3, but to prevent high pH in effluent, Utelite should be mixed or layered with gravel. At a 1:10 mass ratio, approximately 650 kg of Utelite and 6500 kg of gravel are required, but Utelite is available in 900 kg increments and this quantity would be considerably more convenient to use. This will result in a slight increase phosphorus removal, but may increase the pH compared to column experiments. The initial effluent pH will likely be above 9, so flushing several pore volumes through the filter bed back to stage 1 is recommended to reduce effluent pH.

With 900 kg of Utelite in each cell, the phosphorus removal capacity of the third stage will be approximately 3.2 kg P. If the second stage effluent P concentration remains at 2.3 mg L^{-1}, the cumulative P removal will decrease to fifty percent of the cumulative input after 14 months. If the effluent concentration rises to 10 mg L^{-1}, this will occur after 3 months. Although the column experiments showed no difference between the mixed

and layered configurations, it is recommended to mix the Utelite with gravel for the initial filling of the cells. When the P removal capacity is saturated, material at influent end of the cell can be removed, and additional Utelite added. The saturated Utelite remaining in the cell may then provide precipitation seed sites, enhancing the long-term P removal.

Several aspects of phosphorus removal are recommended for future research. First, it will be interesting to study the mineralization of the sludge layer in stage 1, and quantify the phosphorus released by this layer over time. Because the phosphorus concentration is critical to both the removal efficiency and the lifespan of filter media, understanding how this concentration may change over time is important. Second, phosphorus removal over the third stage should be monitored to determine adsorption capacity of Utelite under full-scale conditions. This can then be compared to the adsorption capacity under batch and column experiments to determine how well these experiments can predict full-scale performance. The column experiments suggest that removal efficiency is affected by HRT, and so future work should consider the changes in HRT due to the highly variable wastewater flow rate at the ENFH. Lastly, because the filter beds will require periodic replacement of media, it is still worth investigating other potential materials. If an available lower cost material is found with promising phosphorus adsorption capacity, batch tests can be completed quickly and should provide a lower bound for the removal capacity. With three cells in the third stage, different materials can be tested to provide performance comparisons under full-scale conditions.

REFERENCES CITED

Arias, C. A., Brix, H., & Johansen, N.-H. (2003). Phosphorus removal from municipal wastewater in an experimental two-stage vertical flow constructed wetland system equipped with a calcite filter. *Wat. Sci. Tech., 48*(5), 51-58.

Arias, C. A., Del Bubba, M., & Brix, H. (2001). Phosphorus removal by sands for use as media in subsurface flow constructed reed beds. *Wat. Res., 35*(5), 1159-1168.

Bellier, N., Chazarenc, F., & Comeau, Y. (2006). Phosphorus removal from wastewater by mineral apatite. *Water Res, 40*(15), 2965-2971. doi:10.1016/j.watres.2006.05.016

Brown, A. M. (2001). A step-by-step guide to non-linear regression analysis of experimental data using a Microsoft Excel spreadsheet. *Computer Methods and Programs in Biomedicine, 65*(3).

Chazarenc, F., Filiatrault, M., Brisson, J., & Comeau, Y. (2010). Combination of Slag, Limestone and Sedimentary Apatite in Columns for Phosphorus Removal from Sludge Fish Farm Effluents. *Water, 2*(3), 500-509. doi:10.3390/w2030500

Chintala, R., Schumacher, T. E., McDonald, L. M., Clay, D. E., Malo, D. D., Papiernik, S. K., . . . Julson, J. L. (2014). Phosphorus Sorption and Availability from Biochars and Soil/Biochar Mixtures. *CLEAN - Soil, Air, Water, 42*(5), 626-634. doi:10.1002/clen.201300089

Cole, C. V., Olsen, S. R., & Scott, C. O. (1953). The Nature of Phosphate Sorption by Calcium Carbonate. *Soil Science Society of America Journal, 17*(4), 352-356. doi:10.2136/sssaj1953.03615995001700040013x

Comeau, Y., Brisson, J., Réville, J.-P., Forget, C., & Drizo, A. (2001). Phosphorus removal from trout farm effluents by constructed wetlands. *Wat. Sci. Tech., 44*(11-12), 55-60.

Cramer Fish Sciences. (2013). *Montana Rivers and Streams Assessment October 2013*. Retrieved from Lacey, WA:

Cucarella, V., & Renman, G. (2009). Phosphorus sorption capacity of filter materials used for on-site wastewater treatment determined in batch experiments-a comparative study. *J Environ Qual, 38*(2), 381-392. doi:10.2134/jeq2008.0192

Cyrus, J. S., & Reddy, G. B. (2010). Sorption and desorption of phosphorus by shale: batch and column studies. *Water Sci Technol, 61*(3), 599-606. doi:10.2166/wst.2010.861

de Rozari, P., Greenway, M., & El Hanandeh, A. (2016). Phosphorus removal from secondary sewage and septage using sand media amended with biochar in constructed wetland mesocosms. *Sci Total Environ, 569-570*, 123-133. doi:10.1016/j.scitotenv.2016.06.096

Drizo, A., Comeau, Y., Forget, C., & Chapuis, R. P. (2002). Phosphorus Saturation Potential: A Parameter for Estimating the Longevity of Constructed Wetland Systems. *Environ. Sci. Technol., 36*(21), 4642-4648.

Drizo, A., Frost, C. A., Grace, J., & Smith, K. A. (1999). Physico chemical screening of phosphate removing substrates for use in constructed wetland systems. *Wat. Res., 33*(17), 3595-3602.

Drizo, A., Frost, C. A., Grace, J., & Smith, K. A. (2000). Phosphate and ammonium distribution in a pilot-scale constructed wetland with horizontal subsurface flow using shale as a substrate. *Wat. Res., 34*(9), 2483-2490.

Forbes, M. G., Dickson, K. R., Golden, T. D., Hudak, P., & Doyle, R. D. (2004). Dissolved phosphorus retention of light-weight expanded shale and masonry sand used in subsurface flow treatment wetlands. *38*(3), 892-898. doi:10.1021/es034341z

Freeman, J. S., & Rowell, D. L. (1981). The adsorption and precipitation of phosphate onto calcite. *Journal of Soil Science, 32*, 75-84.

Glindemann, D., Edwards, M., Liu, J.-a., & Kuschk, P. (2005). Phosphine in soils, sludges, biogases and atmospheric implications—a review. *Ecological Engineering, 24*(5), 457-463. doi:10.1016/j.ecoleng.2005.01.002

Heistad, A., Paruch, A. M., Vråle, L., Ádám, K., & Jenssen, P. D. (2006). A high–performance compact filter system treating domestic wastewater. *Ecological Engineering, 28*(4), 374-379. doi:10.1016/j.ecoleng.2006.06.011

Hill, C. M., Duxbury, J., Geohring, L., & Peck, T. (2000). Designing constructed wetlands to remove phosphorus from barnyard runoff: A comparison of four alternative substrates. *Journal of Environmental Science and Health, Part A, 35*(8), 1357-1375. doi:10.1080/10934520009377040

Jenssen, P. D., & Krogstad, T. (2003). Design of constructed wetlands using phosphorus sorbing lightweight aggregate (LWA) *Constructed Wetlands for Wastewater Treatment in Cold Climates* (pp. 259-271).

Johansson, L. (1999). Industrial By-Products and Natural Substrata as Phosphorus Sorbents. *Environmental Technology, 20*(3), 309-316. doi:10.1080/09593332008616822

Johansson, L., & Gustafsson, J. P. (2000). Phosphate removal using blast furnace slags and opoka - mechanisms. *Wat. Res., 34*(1), 259-265.

Jung, K. W., Hwang, M. J., Ahn, K. H., & Ok, Y. S. (2015). Kinetic study on phosphate removal from aqueous solution by biochar derived from peanut shell as renewable adsorptive media. *International Journal of Environmental Science and Technology, 12*(10), 3363-3372. doi:10.1007/s13762-015-0766-5

Kadlec, R. H., & Wallace, S. D. (2009). *Treatment Wetlands* (2 ed.). Boca Raton, FL: CRC Press.

Koiv, M., Liira, M., Mander, U., Motlep, R., Vohla, C., & Kirsimae, K. (2010). Phosphorus removal using Ca-rich hydrated oil shale ash as filter material--the effect of different phosphorus loadings and wastewater compositions. *Water Res, 44*(18), 5232-5239. doi:10.1016/j.watres.2010.06.044

Korboulewsky, N., Wang, R., & Baldy, V. (2012). Purification processes involved in sludge treatment by a vertical flow wetland system: focus on the role of the substrate and plants on N and P removal. *Bioresoure Technology, 105*, 9-14. doi:10.1016/j.biortech.2011.11.037

Li, H., Li, Y., Gong, Z., & Li, X. (2013). Performance study of vertical flow constructed wetlands for phosphorus removal with water quenched slag as a substrate. *Ecological Engineering, 53*, 39-45. doi:10.1016/j.ecoleng.2013.01.011

Molle, P., Liénard, A., Boutin, C., Merlin, G., & Iwema, A. (2005). How to treat raw sewage with constructed wetlands: an overview of the French systems. *Water Science and Technology, 51*(9), 11-21.

National Water Quality Monitoring Council. (2003). Water Quality Portal. Retrieved from https://www.waterqualitydata.us/portal/

Nelson, N. O., Agudelo, S. C., Yuan, W., & Gan, J. (2011). Nitrogen and Phosphorus Availability in Biochar-Amended Soils. *Soil Science*, 1. doi:10.1097/SS.0b013e3182171eac

Nilsson, C., Renman, G., Westholm, L. J., Renman, A., & Drizo, A. (2013). Effect of organic load on phosphorus and bacteria removal from wastewater using alkaline filter materials. *Water Res, 47*(16), 6289-6297. doi:10.1016/j.watres.2013.08.001

OECD. (2000). *Test No. 106: Adsorption - Desorption Using a Batch Equilibrium Method*. Paris, France.

Öövel, M., Tooming, A., Mauring, T., & Mander, Ü. (2007). Schoolhouse wastewater purification in a LWA-filled hybrid constructed wetland in Estonia. *Ecological Engineering, 29*(1), 17-26. doi:10.1016/j.ecoleng.2006.07.010

Paing, J., Guilbert, A., Gagnon, V., & Chazarenc, F. (2015). Effect of climate, wastewater composition, loading rates, system age and design on performances of French vertical flow constructed wetlands: A survey based on 169 full scale systems. *Ecological Engineering, 80*, 46-52. doi:10.1016/j.ecoleng.2014.10.029

Paing, J., & Voisin, J. (2005). Vertical flow constructed wetlands for municipal wastewater and septage treatment in french rural area. *Water Sci Technol, 51*(9), 45-55.

Pálfy, T. G., Gourdon, R., Meyer, D., Troesch, S., Olivier, L., & Molle, P. (2017). Filling hydraulics and nitrogen dynamics in constructed wetlands treating combined sewer overflows. *Ecological Engineering, 101*, 137-144. doi:10.1016/j.ecoleng.2017.01.008

Pardo, M. T., Guadalix, M. E., & Garcia-Gonzalez, M. T. (1991). Effect of pH and background electrolyte on P sorption by variable charge soils. *Geoderma, 54*, 275-284.

Prochaska, C. A., & Zouboulis, A. I. (2006). Removal of phosphates by pilot vertical-flow constructed wetlands using a mixture of sand and dolomite as substrate. *Ecological Engineering, 26*(3), 293-303. doi:10.1016/j.ecoleng.2005.10.009

Reddy, K. R., Kadlec, R. H., Flaig, E., & Gale, P. M. (1999). Phosphorus Retention in Streams and Wetlands: A Review. *Critical Reviews in Environmental Science and Technology, 29*(1), 83-146. doi:10.1080/10643389991259182

Rhine, E. D., Sims, G. K., Mulvaney, R. L., & Pratt, E. J. (1998). Improving the Berthelot Reaction for Determining Ammonium in Soil Extracts and Water. *Soil Sc. Soc. Am. J., 62*(2).

Richardson, C. J. (1985). Mechanisms controlling phosphorus retention capacity in freshwater wetlands. *Science, 228*(4706), 1424-1427.

Sarkhot, D. V., Ghezzehei, T. A., & Berhe, A. A. (2013). Effectiveness of biochar for sorption of ammonium and phosphate from dairy effluent. *J Environ Qual, 42*(5), 1545-1554. doi:10.2134/jeq2012.0482

Scholz, F. W. (2004). Maximum Likelihood Estimation *Encyclopedia of Statistical Sciences*: John Wiley & Sons, Inc.

Shilton, A. N., Elmetri, I., Drizo, A., Pratt, S., Haverkamp, R. G., & Bilby, S. C. (2006). Phosphorus removal by an 'active' slag filter-a decade of full scale experience. *Water Res, 40*(1), 113-118. doi:10.1016/j.watres.2005.11.002

Silveira, D. D., Belli Filho, P., Phillipi, L. S., Kim, B., & Molle, P. (2015). Influence of partial saturation on total nitrogen removal in single-stage French constructed wetland treating raw domestic wastewater. *Ecological Engineering, 77*, 257-264. doi:10.1016/j.ecoleng.2015.01.040

Stein, O. R., Towler, B. W., Hook, P. B., & Biederman, J. A. (2007). On fitting the k-C* first order model to batch loaded sub-surface treatment wetlands. *Water Science & Technology, 56*(3), 93. doi:10.2166/wst.2007.515

Stumm, W., & Morgan, J. J. (1996). *Aquatic chemistry: chemical equilibria and rates in natural waters*: Wiley.

Tang, X. Q., Huang, S. L., & Scholz, M. (2009). Comparison of phosphorus removal between vertical subsurface flow constructed wetlands with different substrates. *Water and Environment Journal, 23*(3), 180-188. doi:10.1111/j.1747-6593.2008.00120.x

U.S. EPA. (2016). *National Rivers and Streams Assessment 2008-2009: A Collaborative Survey*. (EPA/841/R-16/007). Washington, D.C.

Vohla, C., Kõiv, M., Bavor, H. J., Chazarenc, F., & Mander, Ü. (2011). Filter materials for phosphorus removal from wastewater in treatment wetlands—A review. *Ecological Engineering, 37*(1), 70-89. doi:10.1016/j.ecoleng.2009.08.003

Vymazal, J. (2007). Removal of nutrients in various types of constructed wetlands. *Sci Total Environ, 380*(1-3), 48-65. doi:10.1016/j.scitotenv.2006.09.014

Vymazal, J., & Kröpfelová, L. (2011). A three-stage experimental constructed wetland for treatment of domestic sewage: First 2 years of operation. *Ecological Engineering, 37*(1), 90-98. doi:10.1016/j.ecoleng.2010.03.004

Xu, N., Chen, M., Zhou, K., Wang, Y., Yin, H., & Chen, Z. (2014). Retention of phosphorus on calcite and dolomite: speciation and modeling. *RSC Advances, 4*(66), 35205. doi:10.1039/c4ra05461j

Yao, Y., Gao, B., Chen, J., & Yang, L. (2013). Engineered biochar reclaiming phosphate from aqueous solutions: mechanisms and potential application as a slow-release fertilizer. *Environ Sci Technol, 47*(15), 8700-8708. doi:10.1021/es4012977

Yao, Y., Gao, B., Zhang, M., Inyang, M., & Zimmerman, A. R. (2012). Effect of biochar amendment on sorption and leaching of nitrate, ammonium, and phosphate in a sandy soil. *Chemosphere, 89*(11), 1467-1471. doi:10.1016/j.chemosphere.2012.06.002

Zhou, M., & Li, Y. (2001). Phosphorus-Sorption Characteristics of Calcereous Soils and Limestone from the Southern Everglades and Adjacent Farmlands. *Soil Sc. Soc. Am. J., 65*, 1404-1412.

Zhu, T., Jenssen, P. D., Maehlum, T., & Krogstad, T. (1997). Phosphorus sorption and chemical characteristics of lightweight aggregates (LWA) - potential filter media in treatment wetlands. *Wat. Sci. Tech., 35*(5), 103-108.

Zoltek, J. (1974). Phosphorus Removal by Orthophosphate Nucleation. *Journal Water Pollution Control Federation, 46*(11), 2496-2520.